PAIRING EFFECTS IN IMPURE LATTICE DYNAMICS

PAIRING EFFECTS IN IMPURE LATTICE DYNAMICS

by

NORMAN JAMES STEWART, B.A.

A Thesis

Submitted to the School of Graduate Studies

in Partial Fulfilment of the Requirements

for the Degree

Master of Science

McMaster University

September, 1976

MASTER OF SCIENCE (1976)   McMASTER UNIVERSITY

(Physics)   Hamilton, Ontario

TITLE: Pairing Effects in Impure Lattice Dynamics

AUTHOR: Norman James Stewart, B.A. (University of Dublin)

SUPERVISOR: Professor D. W. Taylor

NUMBER OF PAGES: v, 84

ABSTRACT

A study is made of the effects of pairing of defects on the dynamics of impure lattices, with the prospect of calculating the properties of crystals with a reasonably high concentration of impurities. A harmonic theory is used, with a mass-defect model, i.e. mass differences only are considered.

Various parameters of lattice dynamics are studied, such as the atomic mean square displacement, by use of the Green's functions of Zubarev (1960), as evaluated by Bruno (1971).

Finally, a calculation is made of the shifts and widths in the phonon spectrum of Copper due to the addition of 20% Gold impurities. The theory of Aiyer et al. (1969) is used, as corrected by Nickel and Krumhansl (1971), with a derivation along the lines of Langer (1961).

It is shown that pairing effects are small and that the high-concentration calculation does not reproduce the experimental results of Svensson and Kamitakahara (1972) so that a more detailed model must be employed, in particular the inclusion of force constant changes and volume effects appears to be necessary.

ACKNOWLEDGMENTS

I would like to thank sincerely my supervisor, Dr. David Taylor, for guiding the course of this work and contributing considerably to its progress.

I also thank the students, staff and Post-Doctoral Fellows of the Theory Group for providing a congenial atmosphere in which to work. In particular, I thank Rob Woodside for being such a good talker, Anup Dutta for being such a good listener and Fred Kus for his excellent numbers.

I would like to thank Mrs. Hazel Coxall for her diligence in turning my random array of pages into this thesis.

Finally I thank my wife, Ruth Wilson, for her support and encouragement during the last year.

TABLE OF CONTENTS

CHAPTER I

THEORY

I.1 GREEN'S FUNCTIONS

I.1a Fundamentals

The Green's functions used throughout this work are those of Zubarev (1960) viz. the so-called double time thermal Green's functions. A convenient definition of these objects is given by;

$$G_A(t,t') = <<A(t) \; ; \; B(t')>>_A$$

$$= + i\theta(t'-t)<[A(t) \; , \; B(t')]> \qquad (1)$$

where A and B are arbitrary operators and the subscript A implies advanced to compare with the retarded Green's function defined by;

$$G_R(t,t') = -i\theta(t-t')<[A(t) \; , \; B(t')]> \; . \qquad (2)$$

A and B are understood to be in the Heisenberg representation, square brackets imply the algebra appropriate to the statistics of the system, commutator in the case of Bosons and anti-commutator in the Fermion case. In addition, pointed brackets imply thermal average over a canonical ensemble, i.e.

$$<A> = \frac{Tr\{e^{-\frac{H}{kT}} A\}}{Tr\{e^{-\frac{H}{kT}}\}} \qquad (3)$$

1

where k is Boltzman's constant, T is the absolute temperature and H is the Hamiltonian operator for the system. The step function, $\theta(t)$ is given by

$$\theta(t) = \begin{cases} 1, & t>0 \\ 0, & t<0 \end{cases} \qquad (4)$$

and is not defined for t=0.

The Green's function behaves as an intermediary between the fundamental dynamical law and the thermally averaged correlation functions

$$<A(t)\ B(t')>$$

of linear response theory. As will be seen presently the correlation function may be readily calculated from the Green's function, which in turn may be found from the dynamical law.

Due to the time independence of the Hamiltonian, a crystal system is invariant with respect to time translations, hence the Green's function can depend on its two time arguments only through their difference;

$$G(t,t') = G(t-t') = G(\tau)$$

implying, for example

$$G_R(t-t')=G_R(\tau) = -i\theta(\tau)<[A(\tau),B(0)] > \qquad (5)$$

$$\text{where } \tau=t-t' \ \ .$$

The use of Fourier transformation greatly simplifies the solution of the equation of motion, so at this point all quantities are time-Fourier transformed, and specializing to bosons,

$$G_R(\omega) = \frac{1}{2\pi} \int_{-\infty}^{\infty} G_R(\tau) \, e^{i\omega\tau} \, d\tau$$

$$= -\frac{i}{2\pi} \int_{-\infty}^{\infty} \theta(\tau) \langle A(\tau)B - BA(\tau) \rangle \, e^{i\omega\tau} \, d\tau \, . \tag{6}$$

Now we use (3) to give

$$\langle A(\tau)B \rangle = \sum_m e^{-\beta\omega_m} \langle m|A(\tau)B|m \rangle / \sum_m e^{-\beta\omega_m} \tag{7}$$

where we have chosen a set of energy eigenstates to sum over, with eigenvalues

$$E_m = \hbar\omega_m \tag{8}$$

with $\quad \beta = \hbar/kT$.

Thence we find;

$$\langle A(\tau)B - BA(\tau) \rangle = \sum_m e^{-\beta\omega_m} \langle m|A(\tau)B - BA(\tau)|m \rangle / \sum_m e^{-\beta\omega_m} \, . \tag{9}$$

Now using the Heisenberg equation of motion

$$A(\tau) = e^{iH\tau/\hbar} \, A(0) \, e^{-iH\tau/\hbar} \tag{10}$$

the right hand side of (9) becomes

$$\sum_{mn} e^{-\beta\omega_m} \{ e^{i(\omega_m - \omega_n)\tau} \langle m|A|n \rangle \langle n|B|m \rangle$$

$$- e^{-i\tau(\omega_m - \omega_n)} \langle m|B|n \rangle \langle n|A|m \rangle \} / \sum_m e^{-\beta\omega_m} \tag{11}$$

Interchanging m and n in the second term leads to

$$\langle A(\tau)B - BA(\tau) \rangle = \sum_{mn} \langle m|A|n \rangle \langle n|B|m \rangle \, e^{-\beta \omega_m} \{ e^{i\tau(\omega_m - \omega_n)}$$

$$- e^{\beta(\omega_m - \omega_n)} e^{-i\tau(\omega_m - \omega_n)} \}/Z \qquad (12)$$

with $Z = \sum_m e^{-\beta \omega_m}$.

Now by defining

$$S(\omega) = \frac{1}{Z} \sum_{mn} \langle m|A|n \rangle \langle n|B|m \rangle \, e^{-\beta \omega_m} \delta(\omega - \omega_{nm}) , \qquad (13)$$

where $\omega_{nm} = \omega_n - \omega_m$, (6) becomes

$$G_R(\omega) = -\frac{i}{2\pi} \int_{-\infty}^{\infty} \theta(\tau) \, e^{i\omega\tau} \, d\tau \int_{-\infty}^{\infty} S(\omega')(1 - e^{-\beta\omega'}) e^{-i\omega'\tau} d\omega' . \qquad (14)$$

It can be seen that

$$\int_{-\infty}^{\infty} S(\omega) \, e^{-i\omega\tau} \, d\omega = \langle A(\tau)B \rangle \qquad (15)$$

hence (14) establishes the connection between the retarded Green's function and the correlation function, and $S(\omega)$ is simply the Fourier transform of the correlation function often called the spectral density function. The relationship can be simplified even further, however, by substituting for $\theta(\tau)$ in (14) using;

$$\lim_{\varepsilon \to 0} \frac{i}{2\pi} \int_{-\infty}^{\infty} \frac{e^{-ix\tau}}{x + i\varepsilon} \, dx = \theta(\tau) \qquad (16)$$

and also

$$\frac{1}{2\pi} \int_{-\infty}^{\infty} e^{ix\tau} \, d\tau = \delta(x) \tag{17}$$

gives

$$G_R(\omega) = \lim_{\varepsilon \to 0} \frac{1}{2\pi} \int_{-\infty}^{\infty} S(\omega') \frac{[1-e^{-\beta\omega'}]}{\omega-\omega'+i\varepsilon} \, d\omega' \tag{18}$$

$$= \frac{1}{2\pi} P \int_{-\infty}^{\infty} \frac{[1-e^{-\beta\omega'}]}{\omega-\omega'} S(\omega') \, d\omega' - \frac{i}{2} [1-e^{-\beta\omega}] S(\omega) \tag{19}$$

where P implies that the integral to be taken is the Principal value integral.

An identical analysis leads to a similar expression for the advanced Green's function, with the sign of the imaginary part reversed. Both Green's functions can thus be represented as branches of the same function, defined over the complex ω plane and given by

$$G(z) = \frac{1}{2\pi} \int_{-\infty}^{\infty} \frac{[1-e^{-\beta\omega'}]S(\omega')}{z-\omega'} \, d\omega' \tag{20}$$

with a cut along the real axis separating G_A in the upper half plane from G_R in the lower half plane, each of which is taken as the limit of vanishingly small imaginary part of ω;

$$G_R = \lim_{\varepsilon \to 0} G(\omega+i\varepsilon)$$

$$G_A = \lim_{\varepsilon \to 0} G(\omega-i\varepsilon) \tag{21}$$

We have thus seen, from (19), that the spectral density is simply related to and may be given by just the imaginary part of the Green's functions. Also the real parts are clearly equal and may be written as

$$\text{Re } G_{R \atop A} = \pm \frac{1}{\pi} P \int_{-\infty}^{\infty} \frac{\text{Im } G_{R \atop A}(\omega') d\omega'}{\omega - \omega'} . \tag{22}$$

Thus knowledge of the imaginary part of either of the Green's functions leads to all possible knowledge of the ensemble averaged properties of the system.

I. 1b Equations of Motion for Lattice Green's Function

Having shown the role played by the Green's function we must now show how it may be evaluated. The approach taken is to use the dynamical law of quantum mechanics in the Heisenberg representation to derive an equation of motion for the Green's function;

$$\frac{dA}{dt} = -\frac{i}{\hbar} [A,H] \tag{23}$$

hence for the Green's function we find

$$\frac{dG_R}{d\tau} = \frac{d}{d\tau} < [A(\tau),B]>(-i\theta(\tau)) \tag{24}$$

$$= -i\delta(\tau)<[A(\tau),B]> - \frac{i}{\hbar} <<[A(\tau),H];B>>_R . \tag{25}$$

Thus we are led to further Green's functions more complicated than the original and exact solution is not generally possible, however in the

present case of the crystal lattice in the Harmonic approximation exact solution is possible as we shall now see.

The correlation function important in this work is the displacement-displacement function, we thus use a Green's function given by

$$G_{\alpha\beta}(\ell,\ell';\tau)_R = \frac{2\pi}{\hbar} <<u_\alpha(\ell,\tau) \; ; \; u_\beta(\ell',0)>>_R \qquad (26)$$

where Greek subscripts imply Cartesian components and the arguments refer to lattice sites.

The equation of motion then gives;

$$\frac{d}{d\tau} G_{\alpha\beta}(\ell,\ell';\tau) = -\frac{2\pi i}{h} \delta(\tau) < [u_\alpha(\ell.\tau), \; u_\beta(\ell',0)] >$$
$$-\frac{2\pi i}{h^2} <<[u_\alpha(\ell,\tau),H]; \; u_\beta(\ell',0)>> . \qquad (27)$$

The Hamiltonian for the lattice in the Harmonic approximation is given by;

$$H = \sum_{\alpha,\ell} \frac{p_\alpha^2(\ell)}{2M_\alpha(\ell)} + \frac{1}{2} \sum_{\substack{\alpha\beta \\ \ell\ell'}} A_{\alpha\beta}(\ell,\ell')u_\alpha(\ell)u_\beta(\ell') . \qquad (28)$$

The system is assumed to consist of a set of atoms located at equilibrium sites ℓ with displacements from that equilibrium given by $u_\alpha(\ell)$ with canonically conjugate momenta in the α direction $p_\alpha(\ell)$. We here assume a Bravais lattice so that each atom is labelled completely by ℓ. The atoms are assumed to perform small and hence simple Harmonic oscillations about this mean position, hence the neglect of higher order terms. The coefficients $A_{\alpha\beta}(\ell,\ell')$ are assumed to be derivable from a potential ϕ, and by simple Taylor expansion are given by;

$$A_{\alpha\beta}(\ell,\ell') = \frac{\partial^2\phi}{\partial u_\alpha(\ell)\partial u_\beta(\ell')} \Big/ u_\alpha(\ell) = u_\beta(\ell') = 0 \ . \tag{29}$$

Now using

$$[u_\alpha(\ell,\tau),H] = i\hbar \frac{d}{dt} u_\alpha(\ell,\tau) = i\hbar \frac{p_\alpha(\ell,\tau)}{M_\alpha(\ell)} \tag{30}$$

where $M_\alpha(\ell)$ is the mass of the atom at site ℓ, and is clearly independent of α, hence we can put

$$\frac{dG_{\alpha\beta}}{d\tau}(\ell,\ell';\tau) = \frac{2\pi}{\hbar M_\alpha(\ell)} \ll p_\alpha(\ell,\tau) \ ; \ u_\beta(\ell',0)\gg \ . \tag{31}$$

Differentiating again leads to:

$$\frac{d^2G_{\alpha\beta}(\ell,\ell';\tau)}{d\tau^2} = \frac{-2\pi}{\hbar M_\alpha(\ell)} i <[p_\alpha(\ell,\tau) \ ; \ u_\beta(\ell',0)> \tag{32}$$

$$- \frac{-2\pi}{\hbar M_\alpha(\ell)} \frac{i}{\hbar} \ll [p_\alpha(\ell,\tau),H] \ ; \ u_\beta(\ell',0)]\gg \tag{33}$$

now using

$$[p_\alpha(\ell,\tau),H] = [p_\alpha(\ell,\tau), \sum_{\substack{\alpha\beta \\ \ell\ell'}} \frac{1}{2} A_{\alpha\beta}(\ell,\ell')u_\alpha(\ell)u_\beta(\ell')] \tag{34}$$

leads to

$$M_\alpha(\ell) \frac{d^2G_{\alpha\beta}(\ell,\ell';\tau)}{d\tau^2} = -2\pi \delta_{(\tau)} \delta_{\alpha\beta}(\ell,\ell') - \sum_{\gamma\ell''} A_{\alpha\gamma}(\ell,\ell'')G_{\gamma\beta}(\ell'',\ell',\tau) \ . \tag{35}$$

To solve the equation of motion, the Green's function is Fourier transformed and for simplicity, mass reduced variables are used;

$$g_{\alpha\beta}(\ell,\ell';\omega) = \sqrt{M_\alpha(\ell)M_\beta(\ell')}\ G_{\alpha\beta}(\ell,\ell';\omega) = M\ G_{\alpha\beta}(\ell,\ell';\omega)$$

(36)

$$a_{\alpha\beta}(\ell,\ell') = \frac{A_{\alpha\beta}(\ell,\ell')}{\sqrt{M_\alpha(\ell)M_\beta(\ell')}} = \frac{1}{M}\ A_{\alpha\beta}(\ell,\ell')$$

(37)

where M is the mass of the (single) atomic species in the pure (Bravais) lattice. This leads to;

$$\omega^2 g_{\alpha\beta}(\ell,\ell';\omega) = \delta(\ell,\ell')\delta_{\alpha\beta} + \sum_{\gamma\ell''} a_{\alpha\gamma}(\ell,\ell'')g_{\gamma\beta}(\ell'',\ell',\omega)$$

(38)

which we can write as $\quad (\omega^2 I - a)g = I$ (39)

$$or \quad g = (\omega^2 I - a)^{-1}.$$ (40)

We have thus a linear algebraic equation to solve instead of a linear second order differential equation. To solve this equation we must diagonalise the force constant matrix, the standard way to achieve this (Born and Huang, 1956) is to perform a spatial Fourier transformation coupled with a transformation to normal co-ordinates. The simplest system on which to perform this transformation is that of a perfect crystal, which is assumed to be of infinite extent and therefore possesses discrete translational symmetry, hence the plane wave analysis. In the case

of the perfect lattice the force constants are simply those relating the species present in the pure crystal. The results of thus transforming the force constant matrix is the dynamical matrix:

$$D^{jj'}(k,k') = \sum_{\substack{\ell\ell' \\ \alpha\beta}} e^{i\underline{k}\cdot\underline{R}_\ell} \sigma_\alpha^j(\underline{k}) \, a_{\alpha\beta}(\ell,\ell') \, e^{-i\underline{k}\cdot\underline{R}_{\ell'}} \sigma_\beta^{j'}(\underline{k}') \qquad (41)$$

the eigenvalues of which are the squares of the normal mode frequencies, hence;

$$\frac{1}{N} \sum_{\substack{\alpha\beta \\ \ell\ell'}} \sigma_\alpha^j(\underline{k}) \, e^{i\underline{k}\cdot\underline{R}_\ell} \, a_{\alpha\beta}(\ell,\ell') \, e^{-i\underline{k}\cdot\underline{R}_{\ell'}} \sigma_\beta^{j'}(\underline{k}') = \delta_{jj'} \, \delta_{kk'} \omega_j^2(\underline{k}) .$$

$$(42)$$

A similar result follows from consideration of the equations of motion;

$$M_\alpha(\ell)\ddot{u}_\alpha(\ell,t) = - \sum_{\ell'\beta} A_{\alpha\beta}(\ell,\ell')u_\beta(\ell',t) . \qquad (43)$$

Time Fourier transformation gives;

$$\omega^2 M_\alpha(\ell)u_\alpha(\ell,\omega) = \sum_{\ell'\beta} A_{\alpha\beta}(\ell,\ell')u_\beta(\ell',\omega) . \qquad (44)$$

Now expressing the atomic displacements in terms of normal co-ordinates with a plane wave variation between unit cells;

$$u_\alpha(\ell,\omega) = \frac{1}{N} \sum_{j\underline{K}} \sigma_\alpha^j(\underline{k}) \, \ell^{i\underline{k}\cdot\underline{R}_\ell} \, u^j(\underline{k}\,\omega) \qquad (45)$$

gives;

$$M_\alpha(\ell)\omega^2 \sum_{j\underline{k}} \sigma_\alpha^j(\underline{k}) \, e^{i\underline{K}.\underline{R}_\ell} \, u^j(\underline{k},\omega) = \sum_{\substack{\ell'\beta' \\ j'\underline{k}'}} A_{\alpha\beta}(\ell,\ell')\sigma_\beta^j(k')$$

$$e^{i\underline{k}'.\underline{R}_{\ell'}} \, u^{j'}(k',\omega) \, . \quad (46)$$

Using the orthonormality of the normal co-ordinates and the plane waves gives;

$$\omega^2 \, u^j(\underline{k}) = \sum_{\substack{j'k' \\ \ell\ell' \\ \alpha\beta}} \frac{1}{M_\alpha(\ell)} A_{\alpha\beta}(\ell,\ell')\sigma_\alpha^{j'}(\underline{k}) \, e^{i\underline{k}.\underline{R}_\ell} \, \sigma_\beta(\underline{k}')$$

$$e^{-i\underline{k}.\underline{R}_{\ell'}} \, u^{j'}(\underline{k},\,\omega) \, . \quad (47)$$

Now, from (41);

$$\sum_{j'\underline{k}'} D^{jj'}(k\underline{k}') \, u^{j'}(\underline{k}',\omega) = \omega^2 \, u^j(\underline{k},\omega) \qquad (48)$$

with ω_j^2 as eigenvalues of the dynamical matrix.

We can thus put;

$$U_\alpha^j(\ell,\underline{k}) = \frac{1}{N} \, e^{i\underline{k}.\underline{R}_\ell} \, \sigma_\alpha^j(\underline{k}) \qquad (49)$$

where $\underset{\sim}{U}$ is the unitary matrix which diagonalises the force constant matrix;

$$\underset{\sim}{U} \, \underset{\sim}{a} \, \underset{\sim}{U}^+ = \underset{\sim}{a}' \qquad (50)$$

such that

$$a'_{jj'}(\underline{kk}') = \delta_{jj'}\, \delta_{\underline{kk}'}\omega^2_j(\underline{k}).$$

(51)

Thus, by transforming equation (38) we find:

$$\underset{\sim}{U}\,\omega^2\,\underset{\sim}{g}\,\underset{\sim}{U}^+ = \underset{\sim}{I} + \underset{\sim}{U}\,\underset{\sim}{a}\,\underset{\sim}{g}\,\underset{\sim}{U}^+$$

(52)

$$\omega^2\underset{\sim}{g}' = \underset{\sim}{I} + \underset{\sim}{a}'\,\underset{\sim}{g}'\,.$$

(53)

Now, in the particular case of perfect crystal lattice dynamics, as we have seen

$$a'_{jj'}(\underline{k},\underline{k}') = \omega^2_j(\underline{k})\delta_{jj'}\delta_{\underline{kk}'}$$

(54)

which leads to

$$p'_{jj'}(k,k',\omega) = \frac{\delta_{jj'}\delta_{kk'}}{\omega^2-\omega^2_j(k)}\,.$$

(55)

Now, by substituting back into

$$\underset{\sim}{p}' = \underset{\sim}{U}\,\underset{\sim}{p}\,\underset{\sim}{U}^+$$

(56)

gives

$$p_{\alpha\beta}(\ell,\ell',\omega) = \frac{1}{N^2}\underset{\substack{jk\\j'\underline{k}'}}{\Sigma}\ e^{-i\underline{k}\cdot\underline{R}_\ell}\ \sigma^{*j}_\alpha(\underline{k})\ p_{jj'}(k,k',\omega)\sigma^{j'}_\beta(\underline{k}')e^{i\underline{k}'\cdot\underline{R}_{\ell'}}$$

(57)

$$P_{\alpha\beta}(\ell,\ell';\omega) = \frac{1}{N2} \sum_{j\underline{k}} \frac{e^{i\underline{k}.(R_{\ell'}-R_{\ell})}}{\omega^2-\omega_j^2(\underline{k})} \sigma_\alpha^{*j}(\underline{k})\sigma_\beta^j(\underline{k}) . \tag{58}$$

In keeping with the 'classical' Green's function method the solution of the non-interacting problem is used as input to solve the interacting problem. In the present context, the place of the interacting problem is taken by a lattice with defects, i.e. foreign atoms substituted for host atoms, or interstitial foreign atoms. Throughout this work a specific model is taken, viz. it is assumed that substitutional impurities only occur, it is also assumed that these atoms differ only in mass from the host atoms, any change in the force constants restraining the defect or host atoms is neglected. Although highly specific, this model is felt to be of some value, as force constant changes may be expected to contribute little more than a perturbation to any effects due to mass change. The equation of motion, (35) for the lattice with mass defects is now written, after Fourier transformation;

$$-\omega^2 M_\alpha(\ell) G_{\alpha\beta}(\ell,\ell';\omega) = -\delta_{\alpha\beta}\delta(\ell,\ell') - \sum_{\gamma\ell''} A_{\alpha\gamma}(\ell,\ell'')G_{\gamma\beta}(\ell'',\ell';\omega) . \tag{59}$$

We now recast this equation in a form as similar as possible to the perfect crystal equation;

$$\omega^2[1-\epsilon(\ell)]M \, G_{\alpha\beta}(\ell,\ell';\omega) = \delta_{\alpha\beta}\delta(\ell,\ell') + \sum_{\gamma\ell''} A_{\alpha\gamma}(\ell,\ell'')G_{\gamma\beta}(\ell'',\ell';\omega) \tag{60}$$

where we define the diagonal matrix ε by:

$$\varepsilon(\ell) = \frac{M - M(\ell)}{M}$$

(61)

where M is the mass of the host crystal. It is clear that ε vanishes unless the site ℓ contains a defect and is also diagonal on $\alpha\beta$. The left hand side of (60) is now brought into the perfect crystal form;

$$\omega^2 G_{\alpha\beta}(\ell,\ell';\omega) = \delta_{\alpha\beta} \delta(\ell,\ell') + \sum_{\gamma\ell''} A_{\alpha\gamma}(\ell,\ell'') G_{\gamma\beta}(\ell'',\ell';\omega)$$

(62)

$$+ \varepsilon(\ell)\omega^2 G_{\alpha\beta}(\ell,\ell';\omega) \delta_{\alpha\beta}.$$

This equation, (62), may be written in matrix notation as;

$$\omega^2 M G = I + A G + V G$$

(63)

where $V_{\alpha\beta}(\ell,\ell';\omega) = \delta_{\alpha\beta}\delta(\ell,\ell') M\varepsilon(\ell)\omega^2$

(64)

$\Rightarrow \qquad [\omega^2 M I - A] G = I + V G .$

(65)

Now, using (40) for the case of the perfect crystal gives

$$P^{-1} G = I + V G$$

(66)

thus

$$G = P + P V G$$

(67)

Equation (67) is the Dyson equation and is valuable because it allows us

to solve the complicated problem of a lattice with defects in two stages.

First, the relatively simple, perfect crystal problem is solved, then the

Green's function for the defect crystal may be calculated and this step

solves the problem. However, a general solution of the Dyson equation

for an arbitrary lattice is not feasible and certain simplifying assump-

tions are necessary. As explained earlier we have already built in the

assumption of mass change only, we shall now see that we are going to

solve the Dyson equation for a pair of mass defects.

I. 2 APPLICATION TO THE PAIR PROBLEM

As found earlier, we must now solve the Dyson equation for

the system consisting of two foreign atoms situated on an otherwise pure

lattice. In general, the perturbation matrix

$$V_{\alpha\beta}(\ell,\ell';\omega) = \varepsilon(\ell)M\omega^2\,\delta_{\alpha\beta}\delta(\ell,\ell') \tag{68}$$

for the mass defect model is clearly diagonal, this being a considerable

simplification and actually makes the problem tractable. In the case

of a force constant change the perturbation matrix is not diagonal and

the resultant coupling of different lattice sites considerably complicates

the problem. Having solved for the pair Green's function, we will proceed

to apply the solution to various parameters of the lattice dynamics;

the mean square displacements for the defect atoms, exploring the dependence

on defect mass and temperature. At each step comparison is made between

the behaviour of a single isolated impurity and one which belongs to a pair.

Finally, the scattering t-matrix is explored and used to obtain the phonon self-energy due to scattering off a pair of defects.

I. 2a Solving the Dyson Equation

We assume a pair of identical defects situated on an otherwise copper lattice so that the perturbation matrix becomes a multiple of the six-dimensional identity:

$$\underset{\sim}{V} = \epsilon M \omega^2 \underset{\sim 6}{I} .\tag{69}$$

We can further break up the Green's function matrix by first projecting onto the defect space, giving a 6×6 matrix, and thus partitioning the result into inter- and intra-defect terms;

$$\underset{\sim}{G} \text{ pair} = \begin{pmatrix} \underset{\sim}{G}(1,1) & \underset{\sim}{G}(1,2) \\ \underset{\sim}{G}(2,1) & \underset{\sim}{G}(2,2) \end{pmatrix}\tag{70}$$

where $G(\ell,\ell')$ are each 3×3 matrices, the arguments of these being the Cartesian components of the defect atoms and their frequency dependence being suppressed. We thus find for the Dyson equation that;

$$\underset{\sim}{G} \text{ pair} = \underset{\sim}{P} \text{ pair} + \underset{\sim}{P} \text{ pair } \epsilon M \omega^2 \underset{\sim}{I} \underset{\sim}{G} \text{ pair}\tag{71}$$

where $\underset{\sim}{P}$ pair is a 6×6 matrix connecting the sites of the defects in the pure crystal, i.e. the perfect crystal Green's function projected onto the defect space. Thus,

$$\underset{\sim}{G} = \underset{\sim}{P} + \epsilon M \omega^2 \underset{\sim\sim}{PG}\tag{72}$$

by analogy with the defect Green's function we partition $\underset{\sim}{P}$:

$$\underset{\sim}{P} \text{ pair} = \begin{pmatrix} P(1,1) & P(1,2) \\ P(2,1) & P(2,2) \end{pmatrix} \tag{73}$$

so we find

$$\begin{pmatrix} \underset{\sim}{G}(1,1) & \underset{\sim}{G}(1,2) \\ \underset{\sim}{G}(2,1) & \underset{\sim}{G}(2,2) \end{pmatrix} = \begin{pmatrix} \underset{\sim}{P}(1,1) & P(1,2) \\ \underset{\sim}{P}(2,1) & \underset{\sim}{P}(2,2) \end{pmatrix}$$

$$+ \varepsilon M\omega^2 \begin{pmatrix} \underset{\sim}{P}(1,1)\underset{\sim}{G}(1,1)+\underset{\sim}{P}(1,2)\underset{\sim}{G}(2,1) & \underset{\sim}{P}(1,1)\underset{\sim}{G}(1,2)+\underset{\sim}{P}(1,2)\underset{\sim}{G}(2,2) \\ \underset{\sim}{P}(2,1)\underset{\sim}{G}(1,1)+\underset{\sim}{P}(2,2)\underset{\sim}{G}(2,1) & \underset{\sim}{P}(2,1)\underset{\sim}{G}(1,2)+\underset{\sim}{P}(2,2)\underset{\sim}{G}(2,2) \end{pmatrix} \tag{74}$$

we can write this matrix equation as four simultaneous equations:

$$\underset{\sim}{G}(1,1)=\underset{\sim}{P}(1,1)+V\underset{\sim}{P}(1,1)\underset{\sim}{G}(1,1)+V\underset{\sim}{P}(1,2)\underset{\sim}{G}(2,1) \tag{75a}$$

$$\underset{\sim}{G}(1,2)=\underset{\sim}{P}(1,2)+V\underset{\sim}{P}(1,1)\underset{\sim}{G}(1,2)+V\underset{\sim}{P}(1,2)\underset{\sim}{G}(2,2) \tag{75b}$$

$$\underset{\sim}{G}(2,1)=\underset{\sim}{P}(2,1)+V\underset{\sim}{P}(2,1)\underset{\sim}{G}(1,1)+V\underset{\sim}{P}(2,2)\underset{\sim}{G}(2,1) \tag{75c}$$

$$\underset{\sim}{G}(2,2)=\underset{\sim}{P}(2,2)+V\underset{\sim}{P}(2,1)\underset{\sim}{G}(1,2)+V\underset{\sim}{P}(2,2)\underset{\sim}{G}(2,2) \tag{75d}$$

where $V = \varepsilon M\omega^2$.

We now proceed to solve these simultaneous equations. First note that due to the cubic symmetry of the perfect copper lattice, the

three Cartesian directions are independent, hence the Green's function can have no elements linking different Cartesian directions of the same atom, thus $\underset{\sim}{P}(1,1)$ and $\underset{\sim}{P}(2,2)$ are diagonal, also, due to cubic symmetry, the three Cartesian axes are symmetry related and thus

$$\underset{\sim}{P}(1,1) = P1\underset{\sim 3}{I} . \tag{76}$$

Also, a member of the space group of the crystal can be found which transforms any atom into any other atom, hence we require

$$\underset{\sim}{P}(1,1) = \underset{\sim}{P}(2,2) = P1\underset{\sim 3}{I} \tag{77}$$

$$P(\ell,\ell') = P(\ell',\ell) \tag{78}$$

$$\underset{\sim}{P}(1,2) = \underset{\sim}{P}(2,1) .$$

We have thus simplified the simultaneous equations to be solved to;

$$\underset{\sim}{G}(1,1) = P1\underset{\sim 3}{I} + VP1\underset{\sim}{G}(1,1) + V\underset{\sim}{P}(1,2)\underset{\sim}{G}(2,1) \tag{79a}$$

$$\underset{\sim}{G}(1,2) = \underset{\sim}{P}(1,2) + VP1\underset{\sim}{G}(1,2) + V\underset{\sim}{P}(1,2)\underset{\sim}{G}(2,2) \tag{79b}$$

$$\underset{\sim}{G}(2,1) = \underset{\sim}{P}(2,1) + V\underset{\sim}{P}(2,1)\underset{\sim}{G}(1,1) + VP1\underset{\sim}{G}(2,1) \tag{79c}$$

$$\underset{\sim}{G}(2,2) = P1\underset{\sim 3}{I} + V\underset{\sim}{P}(2,1)\underset{\sim}{G}(1,2) + VP1\underset{\sim}{G}(2,2) . \tag{79d}$$

Looking at the form of these equations we see that they have decoupled naturally into two pairs, a with c and b with d, these pairs have identical structures and each may be represented formally by;

$$\underset{\sim}{A} = P1\underset{\sim 3}{I}+VP1\underset{\sim}{A}+V\underset{\sim}{P}(1,2)\underset{\sim}{B}$$

(80)

$$\underset{\sim}{B} = \underset{\sim}{P}(1,2)+V\underset{\sim}{P}(1,2)\underset{\sim}{A}+VP1\underset{\sim}{B}$$

to get equations a and c we replace $\underset{\sim}{A}$ and $\underset{\sim}{B}$ by $\underset{\sim}{G}(1,1)$ and $\underset{\sim}{G}(2,1)$ respectively, to get equations b and d we replace $\underset{\sim}{A}$ and $\underset{\sim}{B}$ with $\underset{\sim}{G}(2,2)$ and $\underset{\sim}{G}(1,2)$. Thus we have found that

$$\underset{\sim}{G}(1,2) = \underset{\sim}{G}(2,1)$$

(81)

$$\underset{\sim}{G}(1,1) = \underset{\sim}{G}(2,2).$$

We now need solve only two simultaneous equations,

$$\underset{\sim}{G}(1,1)=P1\underset{\sim 3}{I}+VP1\underset{\sim}{G}(1,1)+V\underset{\sim}{P}(1,2)\underset{\sim}{G}(1,2)$$

(82a)

$$\underset{\sim}{G}(1,2)=\underset{\sim}{P}(1,2)+VP1\underset{\sim}{G}(1,2)+V\underset{\sim}{P}(1,2)\underset{\sim}{G}(1,1).$$

(82b)

Solution of these equations gives;

$$\underset{\sim}{G}(1,1)=\left[(1-\epsilon M\omega^2 P1)^2\underset{\sim 3}{I}- (\epsilon M\omega^2)^2\underset{\sim}{P}(1,2)\underset{\sim}{P}(1,2)\right]^{-1}\left[P1(1-\epsilon M\omega^2 P1)\underset{\sim 3}{I}\right.$$

$$\left. + \epsilon M\omega^2\ \underset{\sim}{P}(1,2)\underset{\sim}{P}(1,2)\right]$$

(83a)

$$\underset{\sim}{G}(1,2) = \left[(1-\epsilon M\omega^2 P1)^2\underset{\sim 3}{I}-(\epsilon M\omega^2)^2\underset{\sim}{P}(1,2)\underset{\sim}{P}(1,2)|\right]^{-1}\underset{\sim}{P}(1,2).$$

(83b)

We note immediately that on letting ε go to zero we recover the perfect crystal Green's functions P1 and P(1,2) from $\underset{\sim}{G}(1,1)$ and $\underset{\sim}{G}(1,2)$ respectively. The Green's functions may be compared with that for a single defect, given in the defect-defect case by;

$$G_{\alpha\beta}(1,1) = \frac{P1\delta_{\alpha\beta}}{1-\varepsilon M\omega^2 P1} \quad \text{(Hampson, 1973)} . \tag{84}$$

Further checks on the validity of these Green's functions may be made by numerically computing them with $\varepsilon = 0$ ensuring that the result agrees with the perfect crystal Green's function, this of course provides an efficient check on the programme calculating the pair Green's functions. Also use may be made of the identities (Taylor, 1975)

$$\text{(a)} \quad \frac{2}{\pi} \int_0^\infty \omega \, \text{Im} \, \underset{\sim}{M} \, \underset{\sim}{G} \, d\omega = -\underset{\sim}{I} \quad \text{(b)} \quad \frac{2}{\pi} \int_0^\infty \frac{1}{\omega} \, \text{Im} G(\omega) \, d = -\Phi^{-1} . \tag{85}$$

I.2(b)   Parameters of Pair Effects

We look for an expression for the displacement – displacement correlation function. From (15) and (19) we find

$$<u_\alpha(\ell,\tau)u_\beta(\ell',0)> = \int_{-\infty}^\infty s(\omega) \, e^{-i\omega\tau} \, d\omega$$

$$= \frac{-\hbar}{2\pi} \int_{-\infty}^\infty \frac{2 \, \text{Im} \, G_{\alpha\beta}^R(\ell,\ell';\omega)}{1-e^{-\beta\omega}} \, e^{-i\omega\tau} \, d\omega. \tag{86}$$

To find the mean square displacement we require

$$\langle u_\alpha(\ell) \; u_\alpha(\ell, \tau=0) \rangle = \langle u_\alpha(\ell, \tau \to 0) u_\alpha(\ell) \rangle \tag{87}$$

hence we could use the advanced Green's function, in which case we would have

$$\langle u_\alpha(\ell) u_\beta(\ell, \tau \to 0) \rangle = -\frac{\hbar}{2\pi} \int_{-\infty}^{\infty} e^{-i\omega\tau} e^{-\beta\omega} 2 \mathrm{Im} G_{\alpha\beta}^A(\ell, \ell'; \omega) \, d\omega$$

$$= -\frac{\hbar}{2\pi} \int_{-\infty}^{\infty} e^{-i\omega\tau} \; \frac{2\mathrm{Im} \; G_{\alpha\beta}^R(\ell, \ell'; \omega)}{e^{\beta\omega} - 1} \, d\omega \; . \tag{88}$$

We can recast these integrals in the form of an integral over the positive real numbers; so that (88) becomes

$$\int_{-\infty}^{\infty} \frac{\mathrm{Im} \; \underset{\sim}{G}^R \; e^{-i\omega\tau}}{1 - e^{-\beta\omega}} = \int_{0}^{\infty} \mathrm{Im} \; \underset{\sim}{G}^R(\omega) \coth\left(\frac{\beta\omega}{2}\right) d\omega \tag{89}$$

(Taylor 1975)

on making the transformation $\omega \to -\omega$ and using the fact that $\mathrm{Im} G^R(\omega)$ is an odd function of ω.

Similarly, from (88)

$$\langle u_\alpha(\ell, \tau \to 0) u_\alpha(\ell) \rangle = -\frac{\hbar}{\pi} \int_{0}^{\infty} \mathrm{Im} G_{\alpha\alpha}^R(\ell, \ell; \omega) \coth\left(\frac{\beta\omega}{2}\right) d\omega \tag{90}$$

so the two methods give the same result as required.

As can be seen from equation (83), a pole appears in the Green's

function at the frequency for which

$$\det[(1-\varepsilon m\omega^2 P1)^2 - (\varepsilon M\omega^2)^2 \underset{\sim}{P}(1,2)\underset{\sim}{P}(1,2)]= 0 \cdot \tag{91}$$

In general, this will only occur outside the frequency region in which the density of states of the host crystal, hence the imaginary part of the Green's function, is non-zero. As shown by Taylor (1964) this can occur in the case of a single light defect $(\varepsilon > 0)$ in which case three degenerate pole modes are peeled off the top of the host density of states. It has been shown that these modes are strongly localized on the defect site (Hampson, 1973). In the present case, as we shall see, six local pair modes appear above the host crystal band.

Thus in the case of a light defect care must be taken in evaluating the integral in (90). The residue theorem can be applied immediately to (88), but the fact that poles occur in pairs at frequencies $\pm \omega_0$ complicates the situation, so instead the Dirac identity is applied to e.g. (90), in which a single set of poles occur, giving;

$$<u_\alpha^2(\ell)> = -\frac{\hbar}{\pi} \text{Im} \int_0^\infty \coth\frac{\beta\omega}{2} G_{\alpha\alpha}(\ell,\ell,\omega) \; d\omega$$

$$= -\frac{\hbar}{\pi} \text{Im}(-i\pi)\coth(\frac{\beta\omega_0}{2})\{\text{Residue of } G_{\alpha\alpha}(\ell,\ell;\omega_0)\}$$

$$= +\hbar \coth(\frac{\beta\omega_0}{2})\{\underset{\text{poles}}{\Sigma} \text{ Residue of } G_{\alpha\alpha}(\ell,\ell;\omega_0)\} \cdot \tag{92}$$

Evaluation of the residue is performed numerically making use of the theorem that if a function of the complex variable ω can be expressed in

the form

$$f(\omega) = \frac{p(\omega)}{q(\omega)} \qquad (93)$$

where p and q are analytic function of ω at the pole, then for a first order pole, for which $q'(\omega_0) \neq 0$, the residue of f is given by

$$b_1 = \frac{p(\omega_0)}{q'(\omega_0)} \qquad \text{(Churchill, 1960)} \qquad (94)$$

If the pole is of the second order, and $q'(\omega_0)=0$, but $q''(\omega_0) \neq 0$ then the expression

$$b_1 = 2\frac{p'(\omega_0)}{q''(\omega_0)} - \frac{2}{3}\frac{p(z_0)q'''(z_0)}{[q''(z_0)]^2} \qquad (95)$$

(Churchill, 1960)

must be used. Use of (94) requires that the Green's function be expressed with a non-matrix denominator to which end the relation

$$\underset{\sim}{A}^{-1} = |A|^{-1} \underset{\sim}{ADJA} \qquad (96)$$

where the adjugate of A is given by;

$$(ADJA)_{ij} = (-1)^{i+j} C_{ji} \qquad (97)$$

and C_{ij} is the matrix of cofactors, is invoked. Thus is we express the diagonal components of the Green's function as;

$$G(1,1) = \underset{\sim}{A}^{-1}\underset{\sim}{D} = ADJA*D/\left|\underset{\sim}{A}\right| \tag{98}$$

then the residue is;

$$b_{1\alpha\alpha}(\ell,\ell) = (ADJA*D)_{\alpha\alpha}(\ell,\ell)/\frac{d}{d\omega}\left|A\right|/\omega{=}\omega_0 \ . \tag{99}$$

In order to evaluate the residue it is necessary to find the frequencies at which poles occur. Two approaches to this problem may be taken, the first is to evaluate the determinant involved in (91) and to look for zeros of this function. Clearly this is more advantageous in the present context as it is necessary to find the derivatives of this function at the zeros, and both can be performed simultaneously. Alternatively, the eigenvalue problem can be solved explicitly, i.e. we solve

$$\underset{\sim}{P}(\omega_j^2)\ \underset{\sim}{V}\ \underset{\sim}{u}^j = \underset{\sim}{u}^j \tag{100}$$

which we obtain in the following manner from the equation of motion (44):

$$\omega^2 M(1{-}\varepsilon(\ell))u_\alpha(\ell,\omega) = \underset{\ell'\beta}{\Sigma}\ A_{\alpha\beta}(\ell,\ell')u_\beta(\ell',\omega) \tag{101}$$

where again force constant changes are neglected but their inclusion is straightforward; thus

$$\underset{\ell'\beta}{\Sigma}[\omega^2 M\delta(\ell,\ell')\delta_{\alpha\beta}{-}A_{\alpha\beta}(\ell,\ell')]u_\beta(\ell',\omega) = \varepsilon(\ell)M\omega^2 u_\alpha(\ell',\omega) \tag{102}$$

which, from (40), we see gives

$$\underset{\sim}{u} = \underset{\sim\sim\sim}{PVu} \tag{103}$$

To solve this equation we must transform it so as to diagonalize

the matrix $\underset{\sim}{P}\underset{\sim}{V}$, so we now consider the projection of equation (103)

onto the space of the pair of defects, giving

$$\underset{\sim}{V} = \varepsilon M \omega^2 \underset{\sim}{I} = V \underset{\sim}{I} \tag{104}$$

giving

$$V \underset{\sim}{P} u = \underset{\sim}{u} \tag{105}$$

hence

$$V \underset{\sim}{T}^+ \underset{\sim}{P} \underset{\sim}{T} \underset{\sim}{T}^+ \underset{\sim}{u} = \underset{\sim}{T}^+ \underset{\sim}{u} \tag{106}$$

$$\Rightarrow \quad V P^{jj} u'^j = u'j \tag{107}$$

leading to

$$1 - \varepsilon M \omega^2 P^{jj} = 0 \quad . \tag{108}$$

In the present context, the appropriate transformation is to

symmetry co-ordinates of the pair space. This is a transformation to be

used frequently in the present work as it is clearly the necessary approach

to solving the pair problem. Appendix I discussed the application of

Group theory to the pair problem, for first and second neighbours in a

F.C.C. lattice, appropriate to a Copper host. Projection and transfer

operators (Tinkham, 1964) are used to derive the symmetry co-ordinates

and the transformation is then given by

$$P^{jj'} = \sum_{\substack{\alpha\beta=1,3 \\ \ell\ell'=1,2}} S_\alpha^j(\ell) P_{\alpha\beta}(\ell,\ell') S_\beta^{j'}(\ell') = P^{jj} \delta_{jj'} \quad . \tag{109}$$

The transformed equations (108) now become

A_{1g} $1-\varepsilon M\omega^2\{P_{xx}(1,1) - P_{xx}(1,2)-P_{xx}(1,2)\} = 0$ (a)

B_{2g} $1-\varepsilon M\omega^2\{P_{zz}(1,1) - P_{zz}(1,2)\} = 0$ (b)

B_{3g} $1-\varepsilon M\omega^2\{P_{xx}(1,1) - P_{xx}(1,2)+P_{xx}(1,2)\} = 0$ (c)

B_{1u} $1-\varepsilon M\omega^2\{P_{xx}(1,1) + P_{xx}(1,2) + P_{xx}(1,2)\} = 0$ (d)

B_{2u} $1-\varepsilon M\omega^2\{P_{xx}(1,1) + P_{xx}(1,2) - P_{xx}(1,2) = 0$ (e)

B_{3u} $1-\varepsilon M\omega^2\{P_{zz}(1,1) + P_{zz}(1,2)\} = 0$ (110)

for nearest neighbours((0,0,0) and (1,1,0)) and for

((0,0,0) and (2,0,0)) we find

A_{1g} $1-\varepsilon M\omega^2\{P_{xx}(1,1)-\ell_{xx}(1,2)\} = 0$ (a)

$E_{g(1)}$ $1-\varepsilon M\omega^2\{P_{yy}(1,1)-P_{yy}(1,2)\} = 0$ (b)

$E_{g(11)}$ $1-\varepsilon M\omega^2\{P_{zz}(1,1)-P_{zz}(1,2)\} = 0$ (c)

A_{2u} $1-\varepsilon M\omega^2\{P_{xx}(1,1)+P_{xx}(1,2)\} = 0$ (d)

$E_{u(1)}$ $1-\varepsilon M\omega^2\{P_{yy}(1,1)+P_{yy}(1,2)\} = 0$ (e)

$E_{u(2)}$ $1-\varepsilon M\omega^2\{P_{zz}(1,1)+P_{zz}(1,2)\} = 0.$ (f)

(111)

The equations b and c are clearly identical in the second

neighbour case (2,0,0) as the y and z axes are symmetry related, similarly

e and f are equivalent.

Again, as shown by Taylor (1964), in the case of a heavy defect

($\varepsilon<0$) a Lorentzian resonance appears in the Green's function.   The

frequencies at which the resonances occur are given by (91) and (108)

A further parameter of the effects of pairing in lattice dynamics is given by the optical absorption by charged defects. Taylor (1964) discusses the absorption by a single defect and arrives at the result.

$$\chi_{\alpha\beta}(,k';\omega) = -\frac{N}{V}\frac{e^2}{} G_{\alpha\beta}(k,k';\omega) \tag{112}$$

for the susceptibility χ of the system, consisting of N atoms and occupying volume V. For our purposes, we Fourier transform this relation;

$$\chi_{\alpha\beta}(\ell,\ell';\omega) = -\frac{N e^2}{V} G_{\alpha\beta}(\ell,\ell';\omega) . \tag{113}$$

Now, transforming to symmetry co-ordinates to find the effects due to a single defect pair;

$$\chi^{jj}(\omega) = -\frac{N e^2}{V} G^{jj'} = -\frac{N e^2}{V} G^{jj}\delta(j,j')$$

$$= -\frac{N e^2}{V} \sum_{\substack{\ell\ell'=1,2 \\ \alpha\beta=1,3}} s_\alpha^{j}{}^{*}(\ell) G_{\alpha\beta}(\ell,\ell';\omega) s_\beta^{j'}(\ell') . \tag{114}$$

We also use the relation

$$\alpha^{j}(\omega) = -\frac{4\pi\omega}{mc} \operatorname{Im} \chi^{jj} \tag{115}$$

derived from Maxwell's equation and the fact that the absorption

coefficient α is given by the imaginary part of the complex wave-vector.

We must now sum over optically active symmetry modes to obtain the total absorption. To discover which modes are optically active, we consider the basic relations of the absorption process, firstly, absorption, in the absence of permanent dipoles, is due to an induced dipole moment given by;

$$P_\alpha(k,\omega) = \sum_{\beta k'} \chi_{\alpha\beta}(k,k';\omega) E_\beta(k') \qquad (116)$$

where χ is the susceptibility per unit volume. Spatially Fourier transforming and using (113);

$$P_\alpha(\ell,\omega) = -\frac{N_e 2}{c} \sum_{\beta\ell'} G_{\alpha\beta}(\ell,\ell';\omega) E_\beta(\ell',\omega) E_\beta(\ell',\omega) . \qquad (117)$$

Now the energy absorbed is given by

$$H_I = -\underline{p} \cdot \underline{E} \qquad (118)$$

$$= \frac{N_e 2}{c} \sum_{\substack{\gamma\ell \\ \beta\ell'}} E_\beta(\ell,\omega) G_{\beta\gamma}(\ell,\ell';\omega) E_\gamma(\ell'\omega) \qquad (119)$$

where we have assumed a monochromatic radiation field.

Now we demand that the dipole moment associated with a particular symmetry mode, which we obtain by transforming to symmetry co-ordinates;

$$H_I \propto \underset{\sim\sim\sim}{E} \underset{\sim\sim\sim}{S} S^+ \underset{\sim\sim\sim}{G} S S^+ \underset{\sim}{E} \qquad (120)$$

$$= \underline{E}' \underline{G}' \underline{E}' \qquad (121)$$

$$= \sum_j p^j E' \qquad (122)$$

should transform according to the irreducible representation of the pair symmetry group corresponding to that mode, but the dipole moment transforms as a vector, hence only those modes can acquire a dipole moment whose basis functions transform like vectors. This limits the possible modes in the present context to those of odd symmetry under inversion, i.e. the ungerade modes. This is made quite clear by the simple argument that if the two charged defects are vibrating π out of phase, the dipole moment is identically zero and does not change, thus it is unable to respond to radiation, whereas for motion in phase, the system corresponds to an oscillating charge distribution, thus acquiring a harmonically varying dipole moment. Of course, if the charges on the two defects were of opposite sign the opposite would be the case, viz. the gerade modes would be infra-red active and the ungerade modes not. Also one might expect the gerade modes to be Roman active in the like-charge case. Martin (1967) discusses the absorption by a random array of nearest-neighbour defect pairs, using a simpler model for the Green's functions.

I.3   SECOND ORDER SELF-ENERGY

The most important effect of pairing on lattice dynamics of impure crystals is to evaluate the pair contribution to the self energy which, as we shall see, informs us of the extent to which the phonon frequencies and lifetimes are perturbed due to scattering from defects, and hence gives the modified density of states. Such shifts and widths may be experimentally observed via inelastic neutron scattering.

At the outset one performs an averaging over all configurations of the lattice with defects. This step makes the theory compatible with any experimental work as any real crystal consists of host and defect atoms randomly dispersed, neglecting short range order, so that any given lattice site is equally likely to contain a defect.

When this step is taken, it is clear that translational invariance is restored since all lattice sites are equivalent. We now rewrite the Dyson equation as

$$\langle \underset{\sim}{G} \rangle \ = \ \underset{\sim}{P} \ + \ \underset{\sim}{P} \underset{\sim}{\Sigma} \langle \underset{\sim}{G} \rangle \tag{123}$$

where $\langle \underset{\sim}{G} \rangle$ is the configurationally averaged Green's function, and (123) defines $\underset{\sim}{\Sigma}$, both $\underset{\sim}{\Sigma}$ and $\underset{\sim}{G}$ are now translationally invariant. This then leads to the very important property of $\underset{\sim}{\Sigma}$ that it is diagonal in the $\underset{\sim}{K}$ representation, as are $\underset{\sim}{P}$ and $\langle \underset{\sim}{G} \rangle$. Equation (123) leads to

$$\langle \underset{\sim}{G}(K) \rangle \ = \ \underset{\sim}{P}(K) \ + \ \underset{\sim}{P}(K) \ \underset{\sim}{\Sigma}(K) \ \langle \underset{\sim}{G}(K) \rangle \tag{124}$$

where $\underset{\sim}{P}, \underset{\sim}{\Sigma}$ and $\langle \underset{\sim}{G}(K) \rangle$ are now matrices with respect to the normal mode

co-ordinates. Hence

$$<\underset{\sim}{G}(\underset{\sim}{K})> \;=\; [\underset{\sim}{I}-\underset{\sim}{P}(\underset{\sim}{K})\underset{\sim}{\Sigma}(\underset{\sim}{K})]^{-1}\underset{\sim}{P}(\underset{\sim}{K}) \;=\; [\underset{\sim}{P}^{-1}(\underset{\sim}{K})-\underset{\sim}{\Sigma}(\underset{\sim}{K})]^{-1}$$

$$<G(\underset{\sim}{K})>^{-1}_{jj'} \;=\; (\omega^2-\omega^2_j(\underset{\sim}{K})\delta)_{jj'}-\Sigma^{jj'}(\underset{\sim}{K}) \quad . \tag{125}$$

If $\underset{\sim}{K}$ lies along a symmetry direction it can be shown (Hampson (1973)) that $\underset{\sim}{\Sigma}$ is diagonal with respect to the normal modes thus

$$G^{jj'}(\underset{\sim}{K},\omega) \;=\; \frac{\delta_{jj'}}{\omega^2-\omega^2_j(\underset{\sim}{K})-\Sigma^j(K,\omega)} \quad . \tag{126}$$

$\Sigma^j(\underset{\sim}{K})$ thus acquires the status of a phonon self-energy resulting from defect scattering.

From the quasi-Lorentzian form of Equation (126) we see that the peak in G occurs at

$$\omega^2-\omega^2_j(\underset{\sim}{K})-\text{Re} \; \Sigma^j(\underset{\sim}{K}) \;=\; 0 \tag{127}$$

solving for ω and expanding, assuming Re Σ small,

$$\omega \;=\; \omega_j(\underset{\sim}{K}) + \frac{\text{Re} \; \Sigma^j(\underset{\sim}{K})}{2\omega_j(\underset{\sim}{K})} \quad . \tag{128}$$

Thus the phonon frequency has been shifted by Re $\Sigma^j(\underset{\sim}{K})/2\omega_j(\underset{\sim}{K})$ and similarly we find that the phonons acquire a finite lifetime characterised by the half-width at half-maximum Im $\Sigma^j(\underset{\sim}{K})/2\omega_j(\underset{\sim}{K})$. If Σ were frequency independent we would expect a pure Lorentzian behaviour for G, but in fact Σ shows

interesting structure due to resonant scattering.

We now proceed to derive an expression for $\underset{\sim}{\Sigma}$ via the Dyson equation. The conventional approach is to perform an expansion in the small parameter C, the concentration of defects. Thus we put

$$\underset{\sim}{\Sigma} \quad = \quad c\Sigma^{(1)} + c^2\Sigma^{(2)} + \dots \tag{129}$$

or, in the phonon representation

$$\underset{\sim}{\Sigma}(\underline{K}) \quad = \quad c\underset{\sim}{U} \qquad + c^2\underset{\sim\sim}{U}\Sigma^{(2)}\underset{\sim}{U}^+ \underset{\sim}{\Sigma}^{(1)}\underset{\sim}{U}^+ = c\underset{\sim}{\Sigma}^{(1)}(\underline{K}) + c^2\underset{\sim}{\Sigma}^{(2)}(\underline{K}). \tag{130}$$

Iterating the Dyson equation leads to the infinite series;

$$\underset{\sim}{G} \quad = \quad \underset{\sim}{P} + \underset{\sim\sim}{PVP} + \underset{\sim\sim\sim\sim}{PVPVP} + \dots \quad . \tag{131}$$

Now, in the present mass-defect model, V is diagonal in co-ordinate representation so we find

$$G(\ell,\ell') = \underset{\sim}{P(\ell,\ell')} + V\underset{\ell_1}{\Sigma}P(\ell,\ell_1)P(\ell_1,\ell') + V^2\underset{\ell_1,\ell_2}{\Sigma}P(\ell,\ell_1)P(\ell_1,\ell_2)P(\ell_2,\ell') \tag{132}$$

where P and G are now matrices only with respect to Cartesian components but this fact may be dropped without trouble. It proves convenient in keeping track of terms in this and similar expansions to represent the series diagramatically. In the present context the relevant diagrams are those in

equation (133). A horizontal single line represents a free propagator i.e. the passage of a phonon from one lattice site to another without scattering from a defect and the dotted lines represent a phonon scattering event from a defect site (large dots). Certain well defined rules exist for the construction of a particular series of diagrams so that translation into diagrams allows the summation of the original algebraic series through simple systematic procedures.

$$(133)$$

The diagrams in equation (133) are arranged according to increasing number of interaction lines. A certain simplification is possible immediately by noting the V^2 sum in (132) contains the term for which $\ell_1 = \ell_2$ viz.

$$V^2 \sum_{\ell_1} P(\ell, \ell_1) P(\ell_1, \ell')$$

which can thus be grouped with the term linear in V. Similarly all higher order terms contribute so that the coefficient of $\underset{\sim\sim}{PP}$ becomes the series in (134)

$$(134)$$

$$= V + VP1V + VP1VP1V + \ldots = V/(1-P1V)$$

which we call $t_1(\omega)$, and is the total or dressed interaction of a phonon with a defect site. Our perturbation expansion for $\underset{\sim}{G}$ now becomes

$$G(\ell,\ell') = P(\ell,\ell') + t_1 \sum_{\ell_1} P(\ell,\ell_1) P(\ell_1,\ell')$$

$$+ t_1^2 \sum_{\ell_1 \neq \ell_2} P(\ell,\ell_1) P(\ell_1,\ell_2) P(\ell_2,\ell') + \ldots \qquad (135)$$

The important fact arises that restrictions are placed on the lattice sites in the higher order terms as the excluded terms have been transferred to the preceeding term. As a first approximation in finding the self-energy, one decides to ignore the restrictions after performing a configurational average so that we find

$$G(\ell, \ell) = P(\ell,\ell') + ct_1 \sum_{\ell_1} P(\ell,\ell_1) P(\ell_1,\ell') + c^2 t_1^2 \sum_{\ell_1 \ell_2} P(\ell,\ell_1) P(\ell_1,\ell_2) P(\ell_2,\ell')$$

$$+ \ldots \ldots \qquad (136)$$

where the original summation over defect sites becomes a sum over the entire lattice, with the statistical weighting factor c appearing. It is clear that (136) is simply the iterated form of the equation.

$$\underset{\sim}{G} = \underset{\sim}{P} + ct_1 \underset{\sim}{P} \underset{\sim}{G} \qquad (137)$$

so that we may put

$$\underset{\sim}{\Sigma} = ct_1 \underset{\sim}{I} \qquad (138)$$
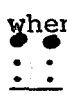
In general one should write equation (135) as

$$\underset{\sim}{G} = \underset{\sim}{P} + \underset{\sim}{P}\underset{\sim}{T}\underset{\sim}{P} \qquad\qquad (139)$$

which equation defines $\underset{\sim}{T}$, the scattering t matrix.

This expression for $\underset{\sim}{\Sigma}$ we know to be incorrect for two reasons. Firstly we ignored the restrictions on the lattice sums in (135) and secondly it is essentially a single site approximation, since we only summed one-defect diagrams in equation (134). It thus neglects pairing effects, in particular diagrams like f, k in (133) have been neglected.

To correct the problem of restricted lattice sums we use the diagrammatic method of Aiyer et al. (1969). The essence of this approach is that one performs the calculation incorrectly and then corrects this expression in a self-consistent fashion. In the single site theory one returns to the expansion of equation (134) and singles out those terms which are given an incorrect statistical weighting.

For example the term $\overset{\bullet}{\underset{\bullet\ \bullet}{\vdots}}$ in the irreducible self-energy gives rise to

terms like $\overset{\cdots}{\cdots}$ in the Green's function expansion when iterated. Now

when a configurational average is performed both sites in the diagram

$\overset{\bullet\ \bullet}{\underset{\cdots}{\cdots}}$ are allowed to range over the whole crystal which means that they

may be the same site, but the term $\overset{\frown}{\smile}$ in the irreducible self energy

already takes this possibility into account so that the term $\overset{\cdot\ \cdot}{\smile}$, where

the curved line implies that the defects connected are to be identified,

must be removed but with a weighting of c^2 since it arises from $\overset{\bullet\ \bullet}{\underset{\cdots}{\cdots}}$ which

has a c^2 weighting. Similarly all diagrams in (134) must be corrected

and we write

$$\Sigma^{(1)} \;=\; \overset{\bullet}{\underset{\cdots}{\vdots}} \;+\; \overset{\bullet}{\triangleq} \;+\; \overset{\bullet}{\triangleq} \;+\;\ldots\ldots$$

$$= V' + P1V'^2 + \ldots = \frac{V'}{1-P1V'} \tag{140}$$

where hatching implies the corrected diagrams and the correction is

formally transferred to V via the prime. We now execute a self-consistent

procedure by assuming we know $\Sigma^{(1)}$ and using it to sum the corrected

diagrams. The corrections are given by Table VIA where the first

column gives the terms going into the first approximation and column n

gives the corrections to these terms which are composed of n irreducible

pieces. The rows are designed to contain only diagrams of the same

TABLE VI

A

B

number of interaction lines, which relation must hold between a diagram and its corrections. As the table implies we have corrected using the corrected irreducible diagrams, thus making the calculation self-consistent. Now summing the entire Table VIA, gives our corrected expression for scattering from a single site. Summation is performed by columns, column 2 for instance gives;

$$\text{column 2} = \quad + \quad + \quad + \quad + $$

$$+ \quad + \quad + \quad + \quad + $$

$$= P1v^{12} + 2P1^2v'^3 + 3P1^3v'^4 + \ldots$$

$$= P1v^{12}/(1-P1v')^2 \tag{141}$$

so that by (140)

$$\text{column 2} = P1 \, \Sigma^{(1)^2} . \tag{142}$$

Similarly column n sums to $P1^{n-1}\Sigma^{(1)n}$. Hence summing all diagrams in Table VIA, which we have said gives $\Sigma^{(1)}$:

$$t_1(\omega) - \Sigma^{(1)^2} P1 - \Sigma^{(1)^3} P1^2 - \ldots = \Sigma^{(1)} \tag{143}$$

leading to

$$\Sigma^{(1)} = \frac{t_1(\omega)}{1+ct_1(\omega)P1} = \frac{V}{1-(1-c)P1V} \tag{144}$$

$\Sigma^{(1)}$ is clearly a multiple of the unit matrix in real space, since all lattice sites are equivalent due to configuration averaging and no inter-defect terms are considered. Thus in the phonon representation, $\Sigma^{(1)}$ is independent of (K,j) and the Fourier transformation is trivial.

Further expanding equation (144) leads to

$$\Sigma^{(1)} \underset{\sim}{\sim} c t_1 - c^2 t_1^2(\omega) P1 \tag{145}$$

so that the correct treatment of single site scattering leads to a second order term in Σ. This term we call $\Sigma^{(2,1)}$.

Our second problem, the treatment of pairs, also gives rise, as we shall see, to a term quadratic in c, which we call $\Sigma^{(2,2)}$. In treating pairs correctly we shall begin by treating them incorrectly, as for the single site, with the approach of Langer (1961). We consider first those irreducible scattering terms for a single isolated pair, in exact parallel with the single site case. This leads to the series in equation (146), where we have considered only those terms beginning on one defect and ending on the other, which thus gives the off diagonal piece of $\Sigma^{(2,2)}$.

$$\Sigma^{(2,2)}_{O.D.} = \quad + \quad + \quad + \ \ldots \ . \tag{146}$$

We are here using solid interaction lines to represent the dressed interaction $t_1(\omega)$ as we must allow any number of separate consecutive scatterings from each defect. Equation (146) gives

$$\Sigma^{(2,2)}_{O.D.}(R) = t_1(\omega) P_2(R) t_1(\omega) P_2(R) t_1(\omega) P_2(R) t_1(\omega) + \ \ldots$$

$$= t_1^4(\omega) P_2^3(R) [1 + a + a^2 + \ldots .]$$

$$= t_1^4(\omega) P_2^3(\underline{R}) [1 - (t_1(\omega) P_2(\underline{R}))^2]^{-1} \tag{147}$$

where $a = (t_1(\omega) P_2(\underline{R}))^2$ and

$$P_2(\underline{R}) = \begin{pmatrix} 0 & P(1,2) \\ P(1,2) & 0 \end{pmatrix}$$

is the propagator taking a phonon from one member of the pair to the other. Because $P_2^2(\underline{R})$ is diagonal with respect to site indices, (147) can be written as

$$\Sigma_{O.D.}^{(2,2)}(\underline{R}) = t_1^4(\omega) P_2^3(\underline{R}) / (1 - [t_1(\omega) P_2(R)]^2) . \tag{148}$$

This is a convenient technique pointed out by Aiyer et al., viz. to regard pair matrices such as $\underset{\sim}{\Sigma}^{(2)}$ as sums of pieces which are multiples of the real Pauli matrices $\underset{\sim X}{\sigma}$ and $\underset{\sim}{I}$:

$$\underset{\sim}{\Sigma}^{(2)} = \Sigma_D^{(2)} \underset{\sim}{I} + \Sigma_{O.D.}^{(2)} \underset{\sim X}{\sigma} \tag{149}$$

with $\qquad \underset{\sim X}{\sigma} = \begin{pmatrix} 0 & 1 \\ 1 & 0 \end{pmatrix}$.

This allows matrix equations to be regarded to an extent as algebraic equations. Now evaluating the diagonal component of $\Sigma^{(2,2)}$ we use

equation (150)

$$\Sigma^{(2,2)}(\underline{R})_{D.} = \text{(diagram)} + \text{(diagram)} + \text{(diagram)} + \dots\dots\dots \tag{150}$$

$$= t_1^3(\omega)P_2^2(\underline{R})/(1-[t_1(\omega)P_2(\underline{R})]^2)$$

We can thus write $\Sigma^{(2,2)}$ as

$$\Sigma^{(2,2)}(\underline{R}) = 1/(1-[t_1(\omega)P_2(\underline{R})]^2\{t_1^3(\omega)P_2^2(\underline{R})\underset{\sim}{I}+t_1^4(\omega)P_2^3(\underline{R})\underset{\sim x}{\sigma}\} \ . \tag{151}$$

Fouriter transforming now leads to

$$\Sigma^{(2,2)}(\underline{K}) = t_1^3(\omega) \sum_{\underline{R}} P_2^2(\underline{R}) \ \{\frac{1+t_1(\omega)P_2(\underline{R})e^{i\underline{K}\cdot\underline{R}}}{1-[t_1(\omega)P_2(\underline{R})]^2}\} \tag{152}$$

after employing translational invariance. Now employing inversion symmetry we find:

$$\Sigma^{(2,2)}(\underline{K}) = 2t_1^3(\omega) \underset{R}{\sum}{}' P_2^2(\underline{R}) \ \{\frac{1+t_1(\omega)P_2(R)\cos\underline{K}\cdot R}{1-[t_1(\omega)P_2(\underline{R})]^2}\} \tag{153}$$

where the prime on the summation implies summation over only half the lattice.

Now adding in $\Sigma^{(2,1)}$ and $\Sigma^{(1)}$ we find

$$\Sigma(\underline{K}) = ct_1(\omega)+c^2[-t_1^2(\omega)P1+2t_1^3(\omega)\underset{\underline{R}}{\sum}{}' P_2^2(\underline{R}) \ \{\frac{1+t_1(\omega)P_2(\underline{R})\cos \ K\cdot R}{1-[t_1(\omega)P_2(\underline{R})]^2}\} \tag{154}$$

At this point we note that our derivation of $\Sigma^{(2)}$ contains the same flaw as our first derivation of $\Sigma_1^{(1)}$, viz. we have performed the configuration averaging incorrectly and wrongly weighted certain diagrams. We thus perform a self-consistent calculation to determine the corrected form exactly as in the single site case. As in the case of $\Sigma^{(1)}$ we write out the corrections in the form of a table, Table VI.

Again the table is summed by columns giving

$$\Sigma(\underline{R}) = ct_1(\omega)/[1+ct_1(\omega)P1 - \frac{c(1-c)t_1^2(\omega)P_2^2(R)}{1-(1-c)t_1P_2(\underline{R})}] \ . \qquad (155)$$

To compare with our previous result we use $[1+A+B\sigma_x]^{-1} \sim 1-A-B\sigma_x$ for small A and B to expand the denominator after rationalising it, giving

$$\Sigma(\underline{R}) \sim ct_1(\omega)\left[1-ct_1(\omega) + \frac{c(1-c)t_1^2(\omega)P_2^2(\underline{R})}{1-(1-c)^2t_1^2(\omega)P_2^2(\underline{R})} + \frac{c(1-c)^2t_1^3(\omega)P_2^3(\underline{R})}{1-(1-c)^2t_1^2(\omega)P_2^2(\underline{R})}\right] \qquad (156)$$

showing that our earlier result was in error by factors of 1-c, as $\Sigma^{(1)}$ had been (equation 144). This expression now refers to the complete self energy to second order, and we note that näively Fourier transforming as suggested by Aiyer et. al., i.e. putting

$$\Sigma(\underline{K}) = \sum_{\underline{R}} [\Sigma_D(\underline{R}) + \Sigma_{O.D.}(\underline{R})e^{i\underline{K}\cdot\underline{R}}] \qquad (157)$$

leads to difficulties as Σ_D is essentially constant as a function of $\underline{R}$ so that $\Sigma(\underline{K})$ becomes proportional to Avogadro's number. To correctly Fourier transform we return to equation (154) and note that $\Sigma^{(2)}(\underline{R})$ i.e. the pure pair second order contribution must be transformed on its own, as pointed out by Nickel and Krumhansl (1971) who write

$$\Sigma(K) = \Sigma^{(1)} + \sum_{R} \Sigma_D^{(2)}(R) + \ldots$$

$$+ \sum_{\underline{R}} \Sigma_{O.D.}^{(2)}(\underline{R})e^{i\underline{K}\cdot\underline{R}} \qquad (158)$$

neglecting higher order terms, where the superscripts now refer to the number of defects being treated in each term and not the exponent of c in that term. Thus the full self-energy must be calculated, first to second order, then to first order and the difference used in the lattice sum.

For computing purposes the method used was to put

$$\underset{\sim}{T}^{(2)} = ct_1\, \underset{\sim}{I} + c^2 t_{\sim PAIR}$$

where $t_{\sim PAIR} =$ $+ \ldots$

$$= t_1^2(\omega) P_2(\underline{R})\, [1 - t_1(\omega) P_2(\underline{R})]^{-1} \qquad (159)$$

hence $\underset{\sim}{T}^{(2)} = ct_1(\omega)\left\{ \underset{\sim}{I} + ct_1(\omega)\begin{pmatrix} 0 & P_2(\underline{R}) \\ P_2(\underline{R}) & 0 \end{pmatrix}\left(I - \begin{pmatrix} 0 & t_1(\omega)P_2(\underline{R}) \\ t_1(\omega)P_2(\underline{R}) & 0 \end{pmatrix}\right)^{-1} \right\}.$

$$(160)$$

This expression is now substituted into

$$\underset{\sim}{\Sigma}(\underline{R}) = \underset{\sim}{T}^{(2)}\, [I + \underset{\sim}{P}\underset{\sim}{T}^{(2)}]^{-1} \quad . \qquad (161)$$

where $\underset{\sim}{\Sigma}$, $\underset{\sim}{T}$ and $\underset{\sim}{P}$ are all 6×6 matrices in the pair subspace. Equation (161) comes very simply from comparing equations 123 and 139 and, in the general case of the whole crystal, is given by

$$\underset{\sim}{\Sigma} = \underset{\sim}{T}[1 + \underset{\sim}{P}\underset{\sim}{T}]^{-1} \quad . \qquad (162)$$

As shown by Aiyer et al. these two methods of deriving the correct self-energy are equivalent.

In conclusion we remark that the differential scattering cross section for single phonon inelastic scattering of thermal neutrons is given by (Bruno (1971))

$$\frac{d^2\sigma}{d\Omega dE} = \frac{a^2 K'}{2\pi K} \frac{e^{\beta\omega}}{e^{\beta\omega}-1} \text{Im} G^j(q,\omega) [\underline{Q}.\underline{\sigma}^j(q)]^2 . \qquad (163)$$

Hence by (126) an experimental examination of the peaks in neutron scattering data gives information on the shifts and widths of phonons in impure crystals. This then allows comparison with calculations from the self energy. Such experiments have been performed by Svensson and Kamitakahara (1971) at a Gold concentration in Copper of 9.3% and the results will be discussed in the following chapter.

CHAPTER II

CALCULATIONS

II. 1a   Green's Functions for the Pair

        The perfect crystal Green's functions used were

those of Bruno (1971), calculated from

$$\nu_{\alpha\beta}(\ell,\ell';\omega) = \frac{V}{(2\pi)^3} \sum_j \int \sigma_\alpha^{*j}(\underline{K})\sigma_\beta^j(\underline{K}) e^{-i\underline{K}\cdot(\ell-\ell')} \delta(\omega_j(\underline{K})-\omega) \, d^3K$$

(164)

which is the generalised density of states, and

$$\text{Im } P_{\alpha\beta}^R(\ell,\ell';\omega) = \frac{\pi}{2\omega} \nu_{\alpha\beta}(\ell,\ell';\omega)$$

(165)

$$\text{Re } P_{\alpha\beta}^R(\ell,\ell';\omega) = -\frac{1}{\pi} P \int_0^{\omega_{MAX}} \frac{\text{Im}P_{\alpha\beta}}{\omega-\omega'} (\ell,\ell';\omega) \, d\omega'.$$

(166)

From these the Green's functions for a defect pair are calculated

as described in I.2. A comparison of the mean square displacement,

which is proportional to Im $G_{\alpha\alpha}(\ell,\ell;\omega)$ by 90, of a heavy defect

to that of a host atom is obtained by plotting Im $MG_{zz}(\ell,\ell;\omega)$ for

a single defect against that for a host atom, as in Fig. 1, which

shows a Gold defect in a Copper lattice with $\varepsilon = -2.1$. The resonance

in the host band is observed, as discussed in I.2b. To find the

effect on the dynamics of a defect atom of adding another defect

nearby, Figs. 2-3 show plots of Im $G_{\alpha\alpha}(0,0;\omega)$ for one member of a

pair, ranging from first neighbour to third, against Im G for a

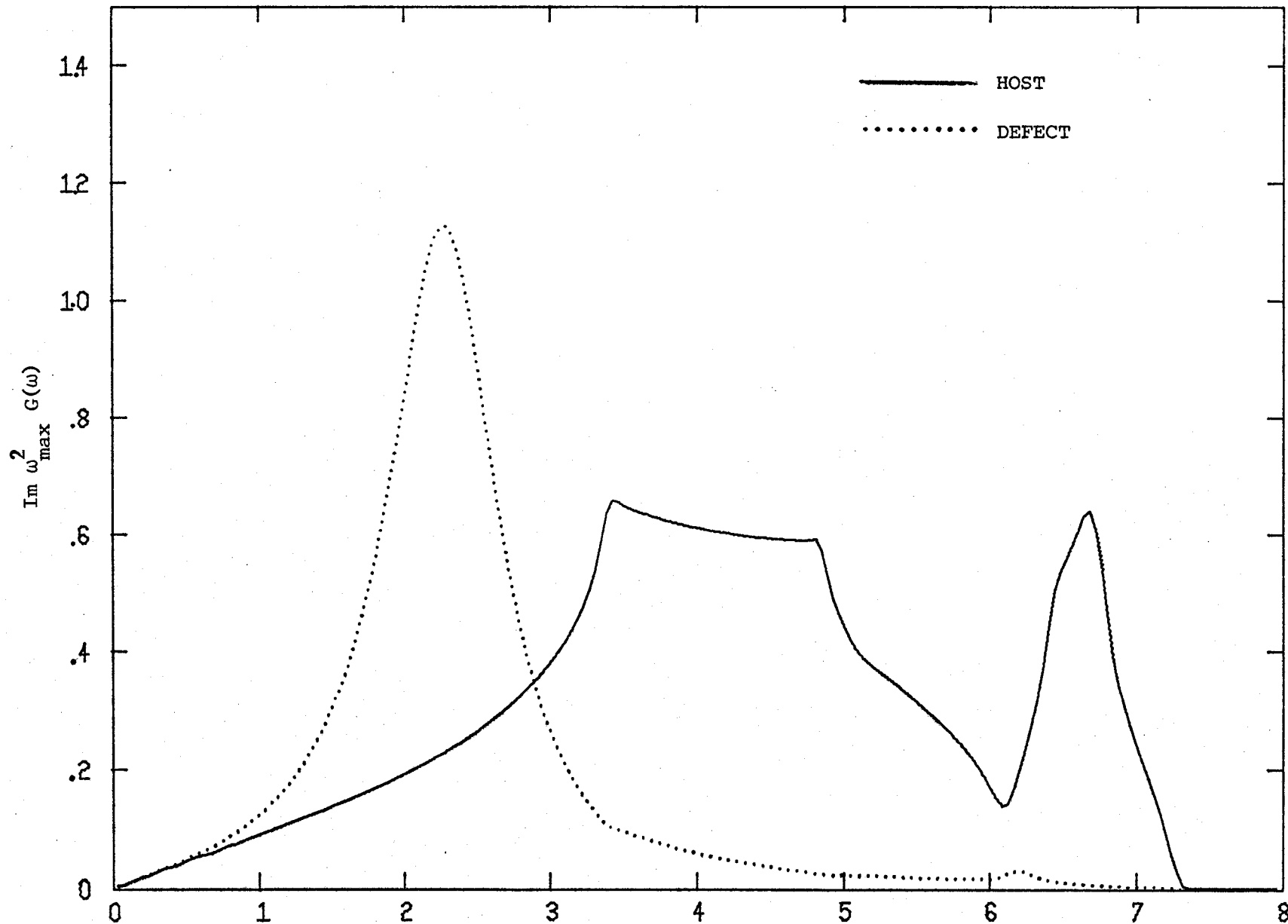single defect. It is seen that any differences, small at first

45

Fig. 1 Im·G(ω)·FOR PURE COPPER AND SINGLE DEFECT WITH ε = -2.1

46

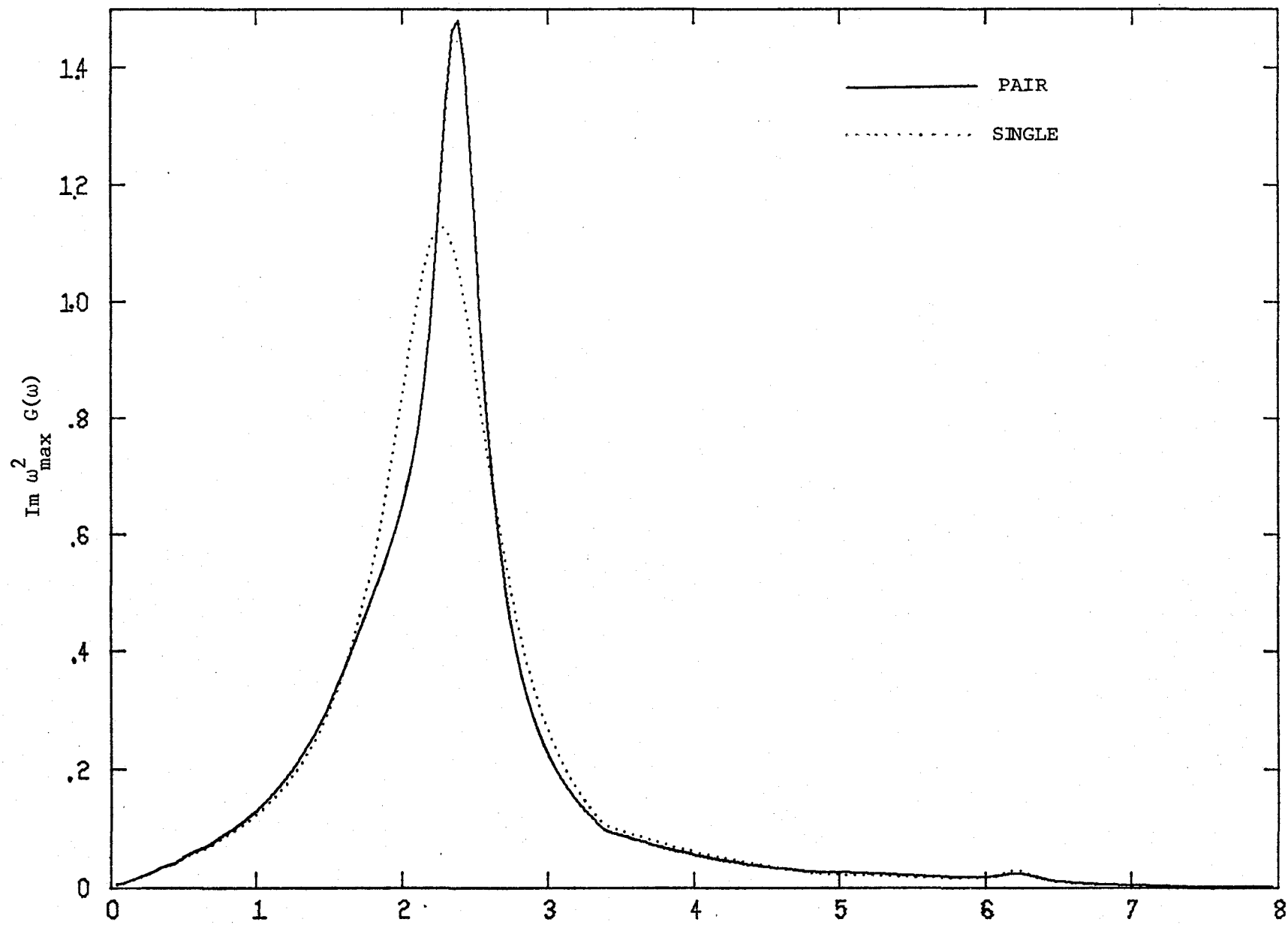Fig. 2   Im G(ω) FOR SINGLE DEFECT AND NEAREST-NEIGHBOUR PAIR, ε = -2.1   THz

47

Fig. 3 Im G(ω) FOR SINGLE DEFECT AND THIRD-NEIGHBOUR PAIR, ε = -2.1   THz

48

neighbour, decay rapidly with separation of the members
of the pair. Possible broadening of the resonance in
the pair case may indicate the splitting of resonant mode frequencies
due to the lifting of degeneracies by the lowered symmetry in the pair
situation. But because of the low density of states of the perfect
crystal at the resonance, the width of the resonance is small, making
structure hard to determine.

For a light defect, I.2b leads us to expect a local mode out-
side the host crystal band, with consequent loss of intensity in the
band. Fig. 4 illustrates this for a single defect, $A\ell$ in Cu with $\varepsilon=.575$.
Figs. 5 - 6 illustrate the similarity between Im G for a single defect
and for a member of a pair. Again the difference is seen to be small.

II 1b Mean Square Displacement

To calculate the mean square displacement the integral over
ω in 90 is performed and a summation over Cartesian directions per-
formed;

$$<u^2(\ell)> = -\frac{\hbar}{\pi} \int_0^\infty \coth(\frac{\beta\omega}{2}) \cdot \Sigma_\alpha \, \text{Im} \, G_{\alpha\alpha}(\ell,\ell;\omega) \, d\omega \; . \qquad (167)$$

In the case of light defects, the pole contribution is calculated
by numerically evaluating the residue at the pole frequencies, to be found
in the next section, as in I.2b. Table I shows a comparison of $<u^2>$ for a
single defect with that for one member of a nearest neighbour pair, for
a range of absolute temperature. We notice the essential mass independence at
high temperatures, which we expect to first order since $\coth(\frac{\beta\omega}{2}) \rightarrow 1/\beta\omega$.

Fig. 4   Im $G(\omega)$ FOR PURE COPPER AND SINGLE DEFECT WITH $\epsilon = .575$

THz

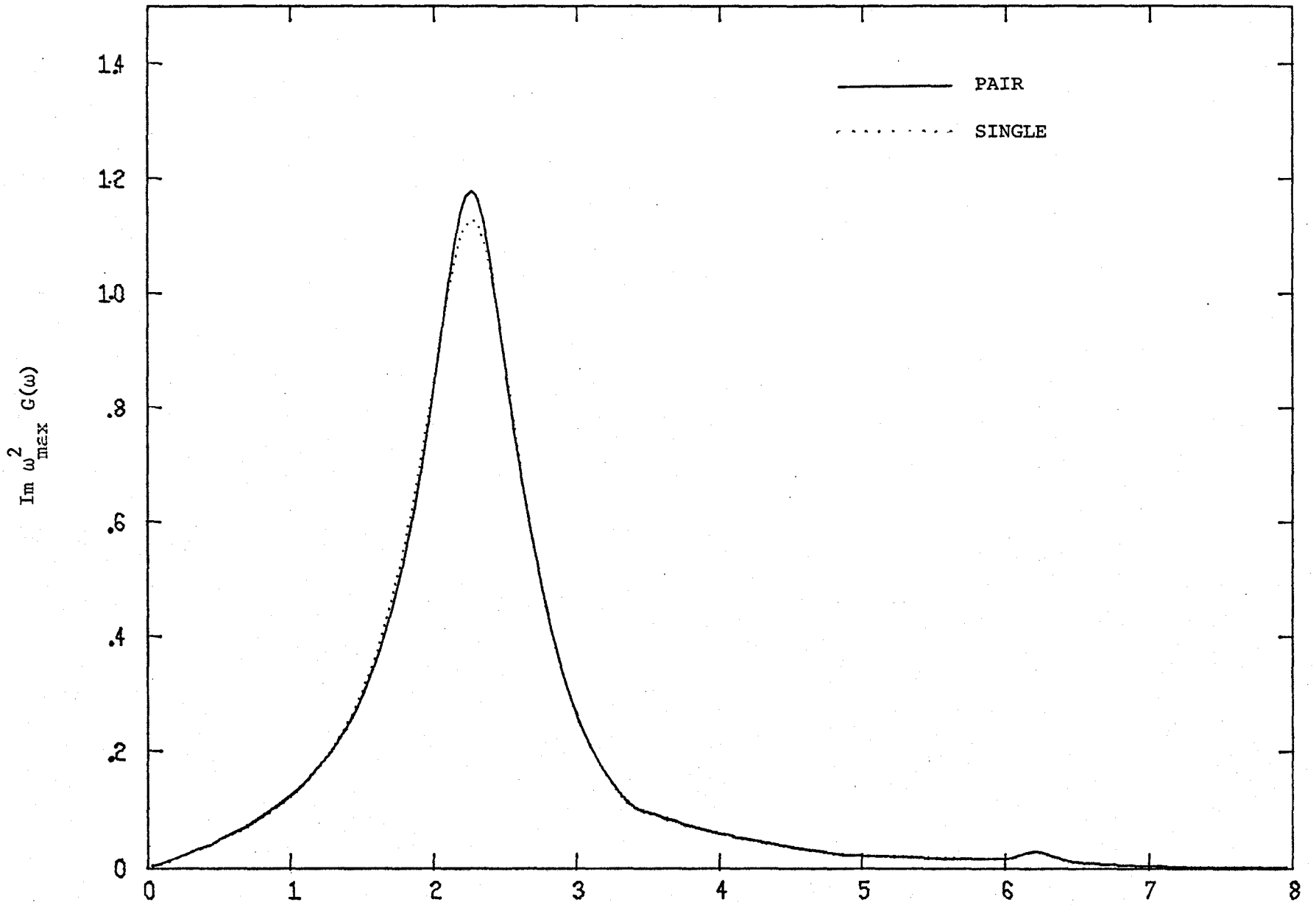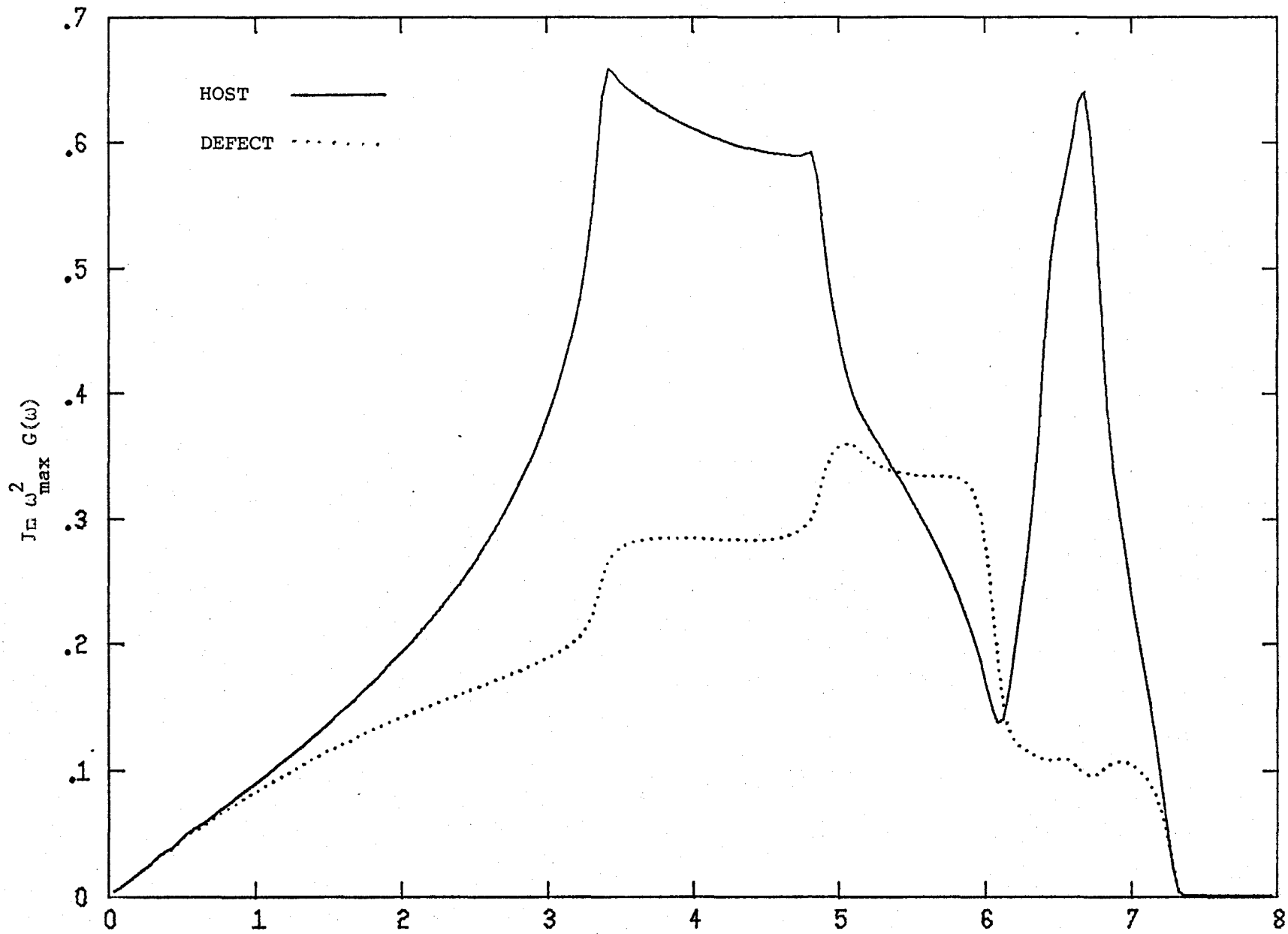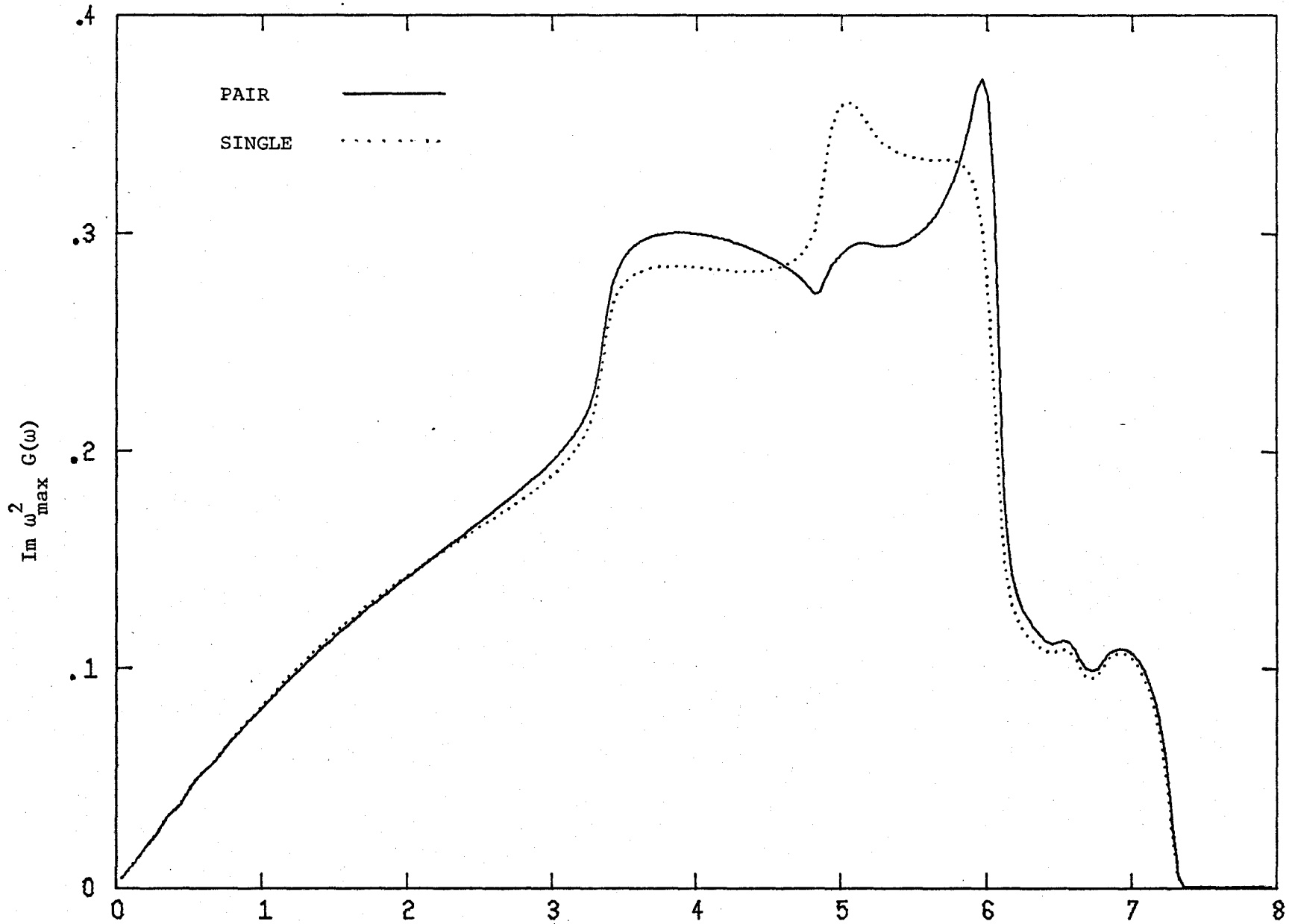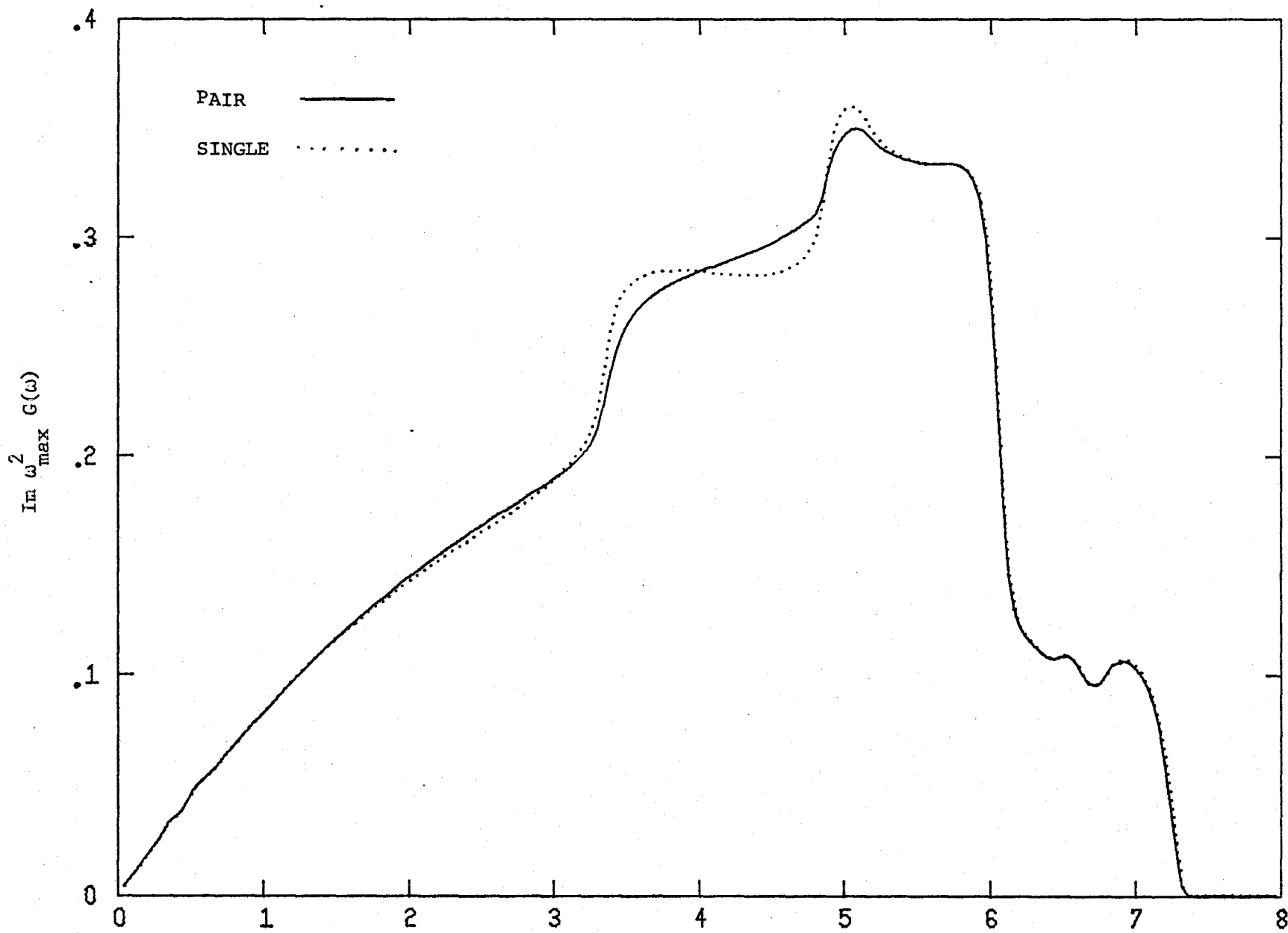Fig. 5   Im G(ω) FOR SINGLE DEFECT AND NEAREST-NEIGHBOUR PAIR, ε = .575

THz

51

Fig. 6   Im G(ω) FOR SINGLE DEFECT AND THIRD-NEIGHBOUR PAIR, ε = .575   THz

52

TABLE I

MEAN SQUARE DISPLACEMENTS

$\epsilon = -2.1$ UNITS OF $10^{-3}(ANG.)^2$

T(K)	$<u^2(\text{SINGLE DEFECT})>$	$<u^2(\text{N.N.PAIR})>$
10	3.2887	3.2942
25	3.5466	3.5452
50	4.5820	4.5828
100	7.5502	7.5511
200	14.2150	14.2158
300	21.0700	21.0709

$\epsilon = .575$

T(K)	LOCAL MODES	BAND	TOTAL	LOCAL MODES	BAND	TOTAL
10	5.0662	3.2463	8.3125	5.0048	3.3316	8.3364
25	5.0662	3.4013	8.4675	5.0048	3.4853	8.4901
50	5.0692	3.8997	8.9690	5.0082	3.9782	8.9863
100	5.2447	5.5000	10.7447	5.1877	5.5690	10.7567
200	6.6013	9.5541	16.1554	6.5441	9.6267	16.1709
300	8.6019	13.8990	22.5010	8.5352	13.9871	22.5223

TABLE II

MEAN SQUARE DISPLACEMENT

T = 50K   UNITS OF 10^{-3}(ANG.)^2

ε = -2.1

RELATIVE ORIENTATION		$\langle u^2 \rangle$
FIRST NEIGHBOUR	(110)	4.5828
SECOND NEIGHBOUR	(200)	4.5833
THIRD NEIGHBOUR	(211)	4.5826
FOURTH NEIGHBOUR	(220)	4.5827
FIFTH NEIGHBOUR	(310)	4.5830
SINGLE DEFECT		4.5820
PERFECT CRYSTAL		6.4105

ε = .575

	LOCAL MODES	BAND	TOTAL
FIRST NEIGHBOUR	5.0082	3.9782	8.9863
SECOND NEIGHBOUR	5.0820	3.8950	8.9770
THIRD NEIGHBOUR	5.0805	3.8875	8.9680
FOURTH NEIGHBOUR	5.0811	3.8771	8.9583
FIFTH NEIGHBOUR	5.0704	3.8974	8.9678
SINGLE DEFECT	5.0692	3.8997	8.9690
PERFECT CRYSTAL	0	6.4105	6.4105

for large T, hence 85(b) , $<u^2>$ tends to a constant value. Table II
shows the dependence on separation between the defects in the pair, again
compared with the single defect values. Again the pair values shows
remarkably little difference from the single defect case. We also note
the large band mode contribution in the nearest neighbour case for Aℓ
defects.

II.2   PAIR MODE FREQUENCIES

To find the frequencies associated with defect pair modes,
the two methods discussed in I.2b were used. The group theory approach was
taken in the case of first and second neighbour pairs. In the second
neighbour case this is necessary as there exist residual degeneracies, in
fact two eigenvalues are doubly degenerate and the irreducible represen-
tations of the symmetry group are useful in characterising these. To
derive these results it was necessary to use the condition that a resonance
occurs only when

$$\frac{d}{d\omega} \omega^2 \text{ Re } G(\omega) < 0 \tag{168}$$

As discussed by Taylor (1975), other values of the frequency
for which the expressions in I.2b are satisfied, but for which 127 is
not satisfied are named "anti-resonances" and do not manifest themselves
physically. Table III shows these ranges of allowed resonance fre-
quencies. The top of the host band in Copper occurs at 7.3THz. Table
IV gives the resonance and local mode frequencies for light and heavy
defects, along with the symmetry of the associated pair mode. We notice

TABLE III

RANGES OF ALLOWED RESONANCE FREQUENCIES

FREQUENCY (THz)	$\frac{d}{d\omega} \omega^2 \mathrm{Re}\ G(\omega)$
$0.92 < \nu < 3.24$	< 0
$3.24 < \nu < 5.0$	> 0
$5.0 < \nu < 6.36$	< 0
$6.36 < \nu < 6.84$	> 0
$6.84 < \nu$	< 0

TABLE IV

57

RESONANCE AND LOCAL MODE FREQUENCIES

	$\varepsilon = .575$		UNITS OF THz
	SYMMETRY	ω_ℓ	ω_R
FIRST NEIGHBOUR	A_{1g}	9.1337	
	B_{2g}	8.3084	
	B_{3g}	8.3580	
	B_{1u}	7.5125	6.012
	B_{2u}	8.5406	
	B_{3u}	8.5807	
SECOND NEIGHBOUR	A_{1g}	8.3797	
	E_g	8.4250	
	A_{2u}	8.5180	
	E_u	8.4781	
	$\varepsilon = -2.1$	ω_R	ω_R
FIRST NEIGHBOUR	A_{1g}	2.7628	6.06
	B_{2g}	2.4460	6.14
	B_{3g}	2.3844	6.396
	B_{1u}	2.3116	-
	B_{2u}	2.9516	6.22
	B_{3u}	2.8628	6.14
SECOND NEIGHBOUR	A_{1g}	2.5348	6.308
	E_g	2.3868	6.148
	A_{2u}	2.5556	6.228
	E_u	2.6838	-
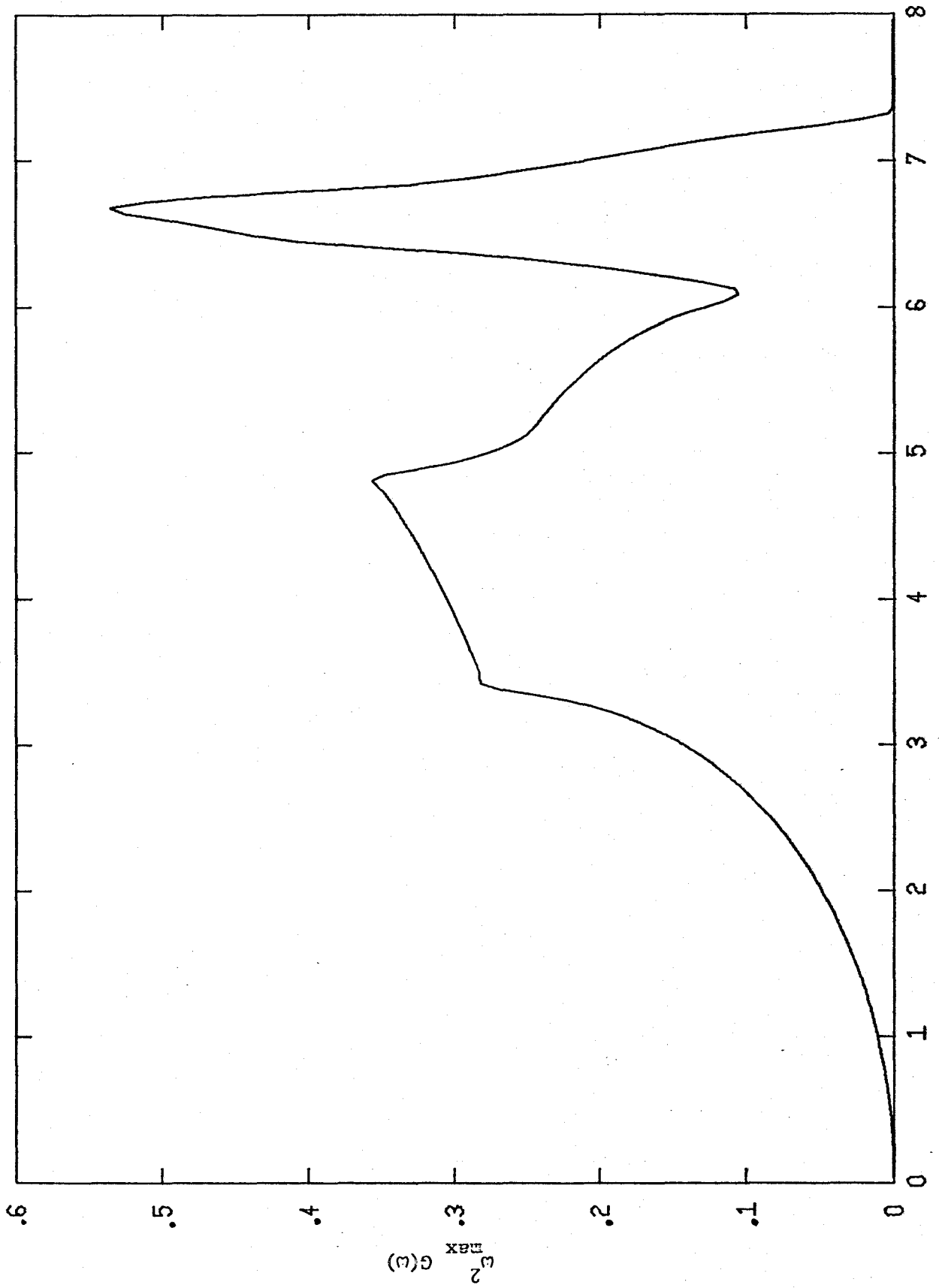
Fig. 7   DENSITY OF STATES FOR PURE COPPER

FIRST

SECOND

THIRD

FOURTH

FIFTH

SINGLE DEFECT

$\overline{0 \cdot 1 T_{Hz}}$
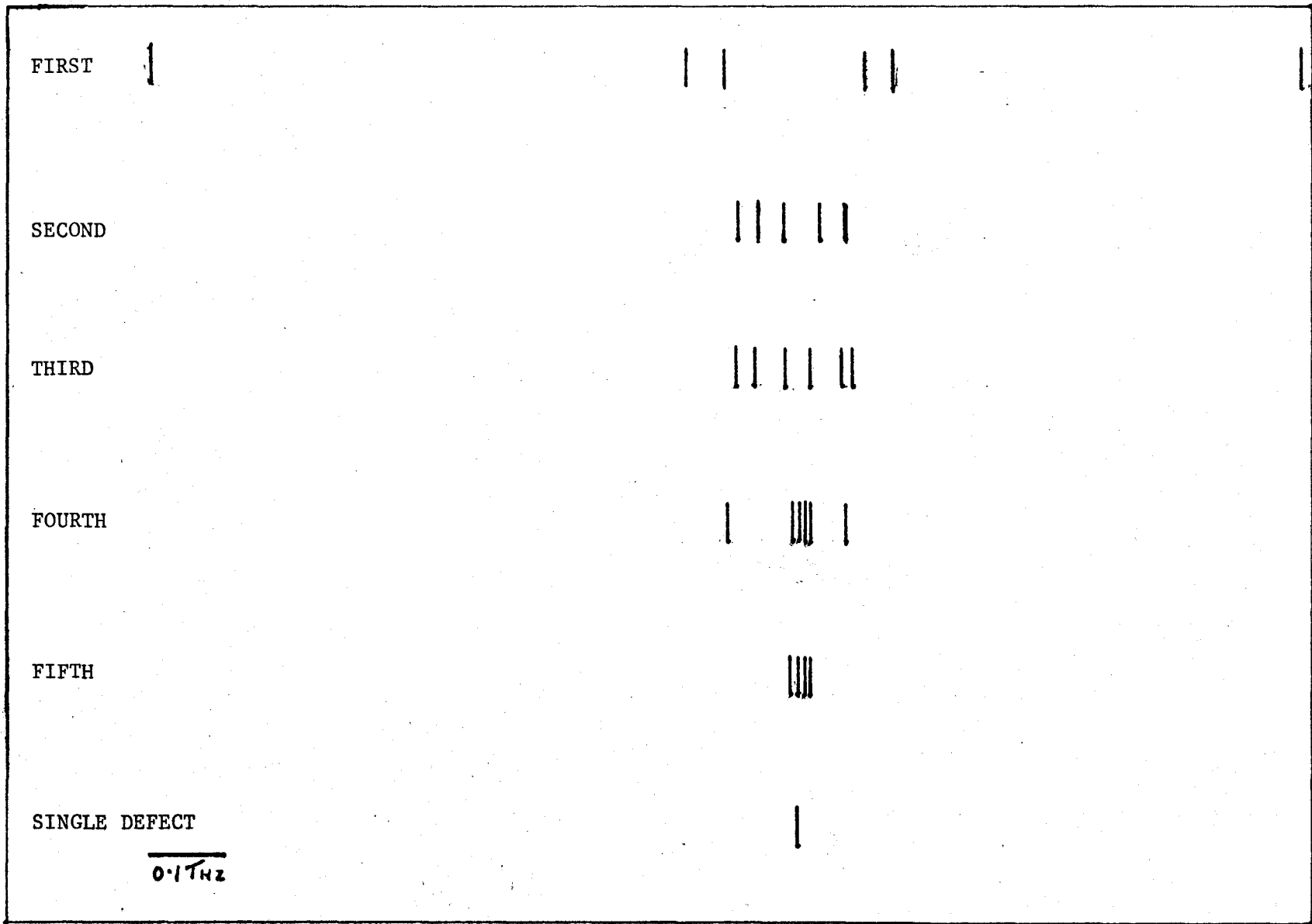
Fig. 8   Local Mode Frequencies

TABLE V

PAIR LOCAL MODE FREQUENCIES (THz.)

$$\varepsilon = .575$$

	ω_ℓ
THIRD NEIGHBOUR	8.3728
	8.3923
	8.4336
	8.4703
	8.5078
	8.5242
FOURTH NEIGHBOUR	8.3704
	8.4412
	8.4495
	8.4550
	8.4631
	8.5241
FIFTH NEIGHBOUR	8.4398
	8.4420
	8.4463
	8 4623
	8.4623
	8.4644

in the light defect case that the mode B_{1u} oscillates at frequencies

above and below the host band to maximum, thus accounting for the large

band mode contribution for a nearest neighbour pair notice in the last

section. By referring to the pure crystal density of states (Fig. 7) we

see that in the light defect case local modes are peeled off the peak near the

top of the Copper band, while the resonance of B_{1u} symmetry is pulled up from

the states below $\nu = 5$ THz. In the heavy defect case, we find two

ranges of resonance frequencies, around 6 THz and below 3 THz. Presumably

these modes are pulled down in frequency from the two peaks in the pure

crystal density of states just mentioned.

Table V gives the local mode frequencies derived from 91 for third

to fifth neighbour defect pairs. We may note the convergence of the local mode

frequencies to the single defect value, almost complete by fifth neigh-

bour and Fig. 8 shows this graphically.

II.3 OPTICAL ABSORPTION

Using the expressions derived in II.2b we calculate the ab-

sorption coefficient for infra-red radiation for a system of randomly oriented

charged defects. Fig. 9 shows the absorption by an alloy of charged

gold atoms in copper which absorb radiation as a single defect i.e. neglecting

pairing effects. Figs.10 and 11 show the expected absorption for nearest

neighbour and second neighbour charged defect pairs, respectively.

These plots exhibit the same qualitative features as the cal-

culation of Martin (1967), who employed a simpler model with which to cal-
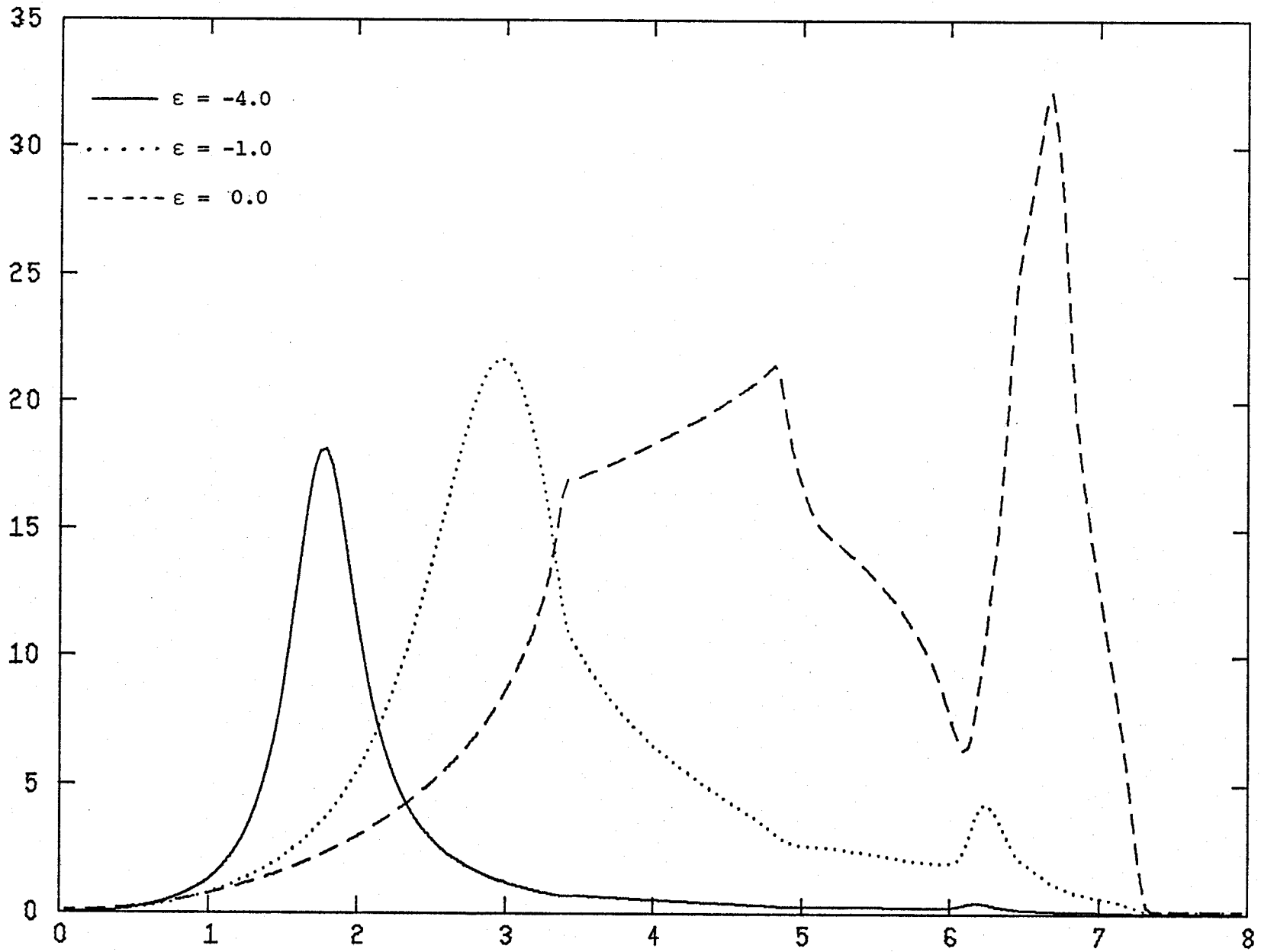
culate the Green's functions for the perfect crystal.

Fig. 9 INFRA-RED ABSORPTION COEFFICIENT FOR RANDOM
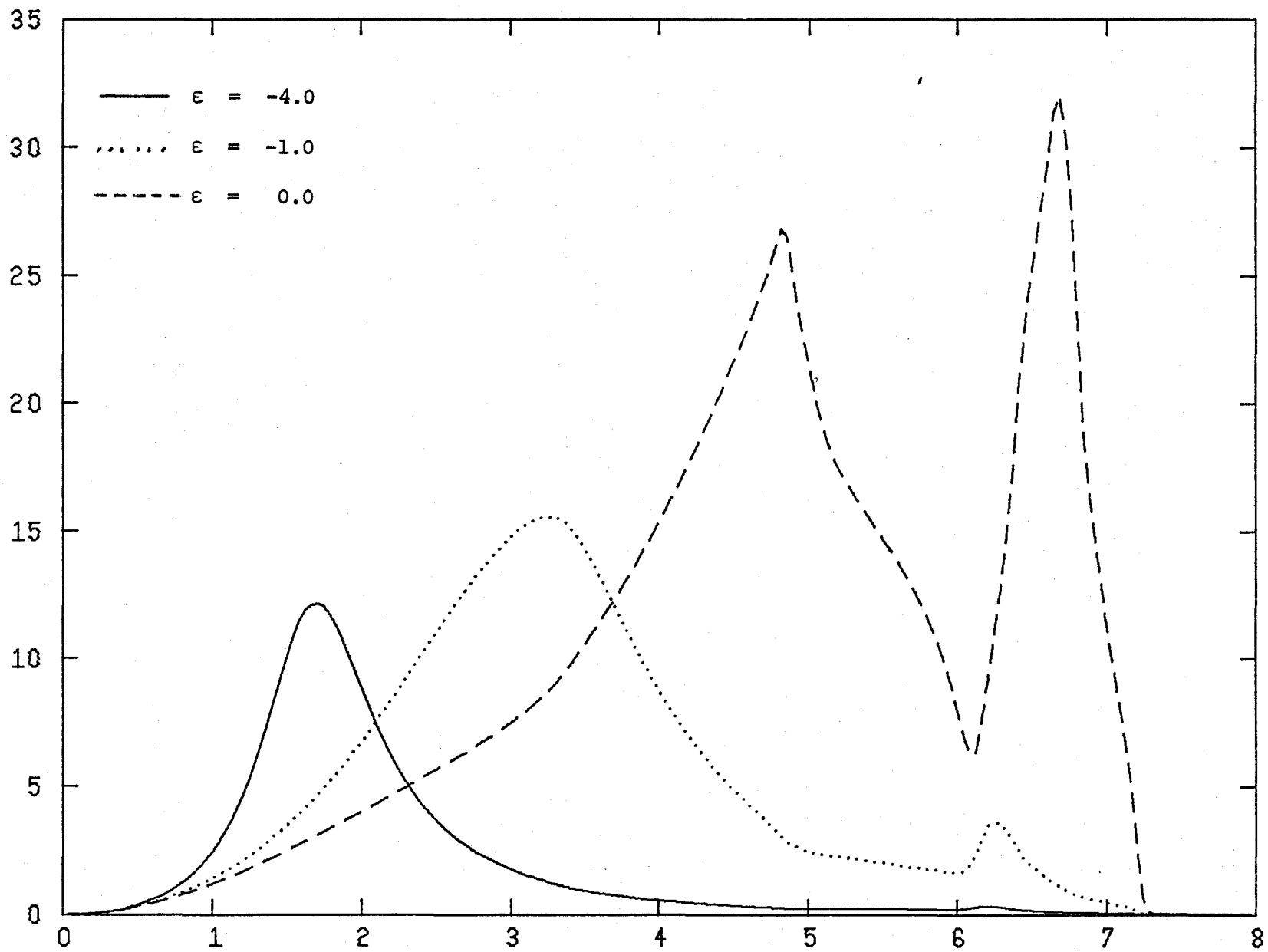
LATTICE OF ISOLATED DEFECTS (ARBITRARY UNITS)

Fig. 10   INFRA-RED ABSORPTION COEFFICIENT FOR RANDOM   THz
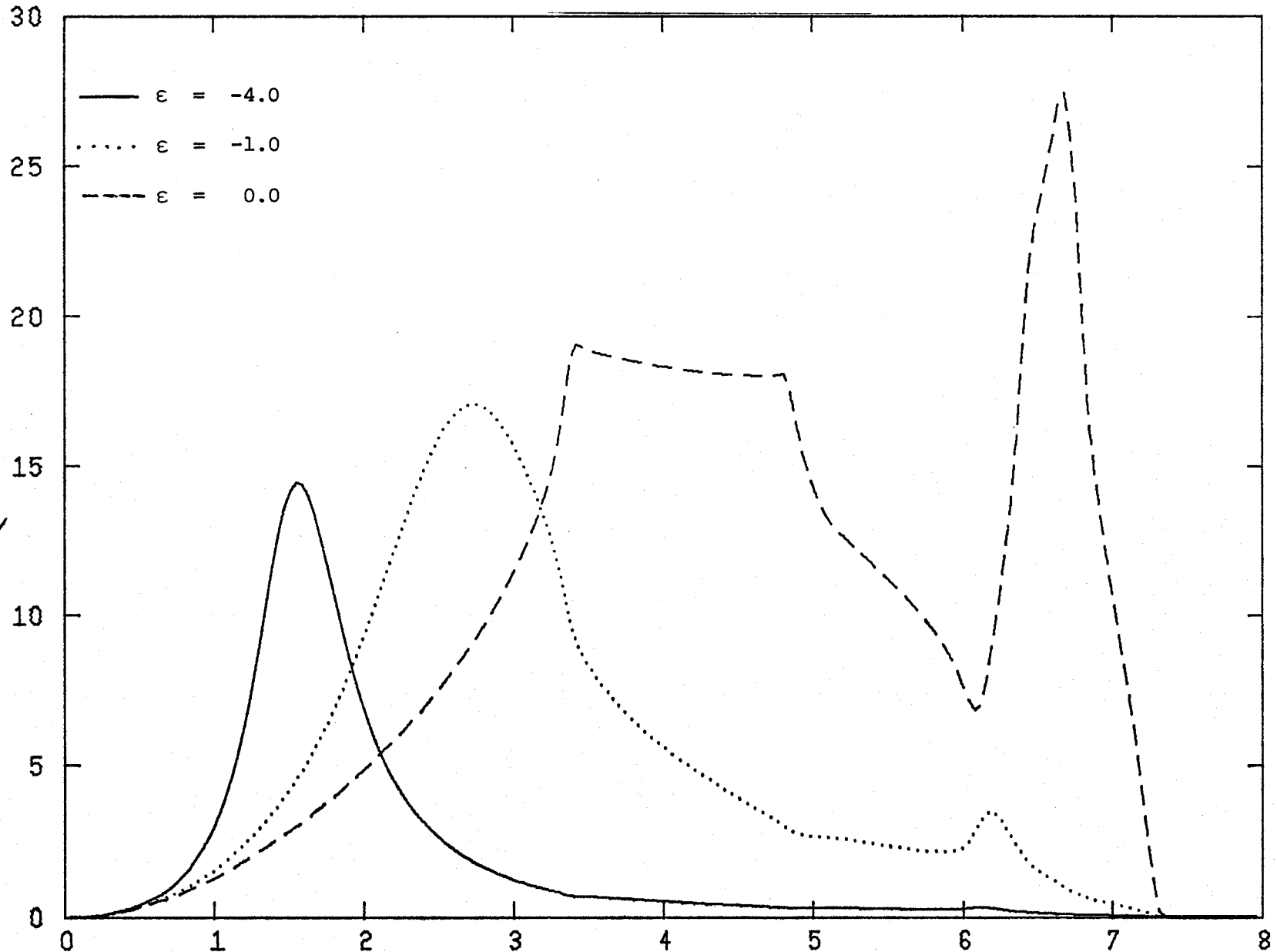   LATTICE OF DEFECT NEAREST-NEIGHBOUR PAIRS

Fig. 11   INFRA-RED ABSORPTION COEFFICIENT FOR RANDOM
LATTICE OF SECOND-NEIGHBOUR DEFECT PAIRS

From the Appendix we see that the absorption coefficient is given, in the nearest neighbour case, after summing our ungerade modes, by

$$\alpha(\omega) \propto \omega \text{Im} \{G_{xx}(1,1) + G_{xx}(1,2) + G_{xy}(1,2)$$

$$+ G_{xx}(1,1) + G_{xx}(1,2) - G_{xy}(1,2) + G_{zz}(1,1) + G_{zz}(1,2)\}$$

$$= \omega \text{Im} \{2G_{xx}(1,1) + 2 G_{xx}(1,2) + G_{zz}(1,1) + G_{zz}(1,2)\}$$

$$\omega \text{Im} \{\text{Tr } \underset{\sim}{G}(1,1) + \text{Tr } \underset{\sim}{G}(1,2)\} \qquad (169)$$

since the x and y axis are symmetry related. We find for the second neighbour case that the result is the same, i.e. α is proportional to the sum of the traces of the inter and intra defect Green's functions.

II.4 PHONON SHIFTS AND WIDTHS

To perform the Fourier transformation discussed in section I.3 certain symmetry directions in K space were chosen viz. the (111),(110) and (100) directions. Σ may now be regarded as diagonal so that a single $(j,\underline{K})$ pair specifies it. From equation 154 it is noted that a sum is necessary over half the lattice; of course this is impossible in practice so that only certain shells of the closest neighbours are chosen. In the present work the calculation was performed out to fifth neighbout but little difference accrued on summing beyond second neighbours, so that the major effects were due to nearest and second neighbours. Fig. 19 illustrates the convergence, showing the on-shell shifts summed to first, second and fifth neighbour shells. This verifies the assumed convergence of the sum and validates the approximation of terminating the sum.

The sum to be performed is rewritten as;

$$\Sigma^{(2)}(\underline{K}) = \sum_{n} \sum_{\underline{R}}{}' \underset{\sim}{S}^{+} \Sigma_{\sim n} \underset{\sim}{S}(\underline{R}) \cos \underline{K} \cdot \underline{R} \qquad (170)$$

where $\underset{\sim}{S}(\underline{R})$ is a notation matrix which is a representative of a member of the point group of the crystal and notates Σ_{n} for a given lattice site into that for another lattice site at the same distance from the origin, thus $\underset{\sim}{\Sigma}(\underline{R})$ need only be known for one site in each shell, and the sum over n implies summation over shells. Now further transforming to phonon modes gives;

$$\Sigma^{(2)j}(\underline{K}) = \sum_{n} \sum_{\underline{R}}{}' \underset{\sim}{\sigma}^{*j} \underset{\sim}{S}^{+}(\underline{R}) \underset{\sim}{\Sigma} \underset{\sim}{S}(\underline{R}) \underset{\sim}{\sigma}^{j} \cos(\underline{K} \cdot \underline{R}) \qquad (171)$$

Now we note that it is only necessary to evaluate the column matrix

$$\underset{\sim}{A}^j(R) = \underset{\sim}{S}(R)\underset{\sim}{\sigma}^j \qquad\qquad (172)$$

for each $\underline{R}$ and j so instead of performing matrix multiplication only

matrices and vectors need be multiplied:

$$\Sigma^{(2)j}(\underline{K}) = \underset{n}{\Sigma} \underset{\underline{R}}{\Sigma} {}' A^{*j}(\underline{R}) \underset{n}{\Sigma} A^j(\underline{R}) . \qquad\qquad (173)$$

The results of these calculations appropriate for gold impurities in copper are shown in Figs. 12-15. Figs. 12 and 13 show the calculated frequency shifts for the L(110) and T(111) phonon modes at C = 20%. These shifts are "on-shell", i.e. they are plotted against the host phonon frequency, so that it is necessary to calculate $\Sigma^j(\underline{K},\omega)$ at several points in K space and then evaluate $\omega_j(\underline{K})$ for the perfect copper crystal and choose the corresponding frequency at each K value. In these illustrations we have plotted the single site approximation to Σ (solid line) and the second order calculation (discrete points). It is important to note that the single site calculation contains $\Sigma^{(2,1)}$, the first second order correction so that the difference between the two plots is just pairing effects. The largest effects obtained among all nine phonon modes along symmetry directions are those illustrated, although variation between modes was very small. Figs. 14 and 15 illustrate the half widths corresponding to Figs. 12 and 13.

As we can see pairing effects contribute little to the phonon shifts and widths. Any effects there are tend to strengthen the resonant behaviour, sharpening the resonant jump in the shift and increasing the

resonant widths.

Figs. 16-19 illustrate experimental determinations of shifts
and widths at a gold concentration of 9.3%. It is clear that pairing
effects are too small to be the cause of the observed effects. In fact
we see for the L(100) case that the resonant behaviour has been complete-
ly lost.

It is thus apparent that the mass defect model, even calculated
to second order in the defect concentration is unable to give the ob-
served phenomena, hence one must turn to alternative causes, notably
force constant changes and volume changes. Force constant changes have
been considered by Bruno (1971), Hampson (1973) and Woodside (1976)
by fitting force constant changes to elastic constant measurements.
These results were also unable to reproduce the phenomena, although
several errors have been found in that work by Woodside (1976). The
effects of volume changes is as yet an unsolved problem and the
current approach is to include volume changes via the mode Gruneisen
parameter. Again the theory is insufficient so that the dynamics of
lattices with a high concentration of defects remains a problem to be
solved. What we can infer from the present work is the positive result
that the solution does not lie in the pairing effects of mass defects.
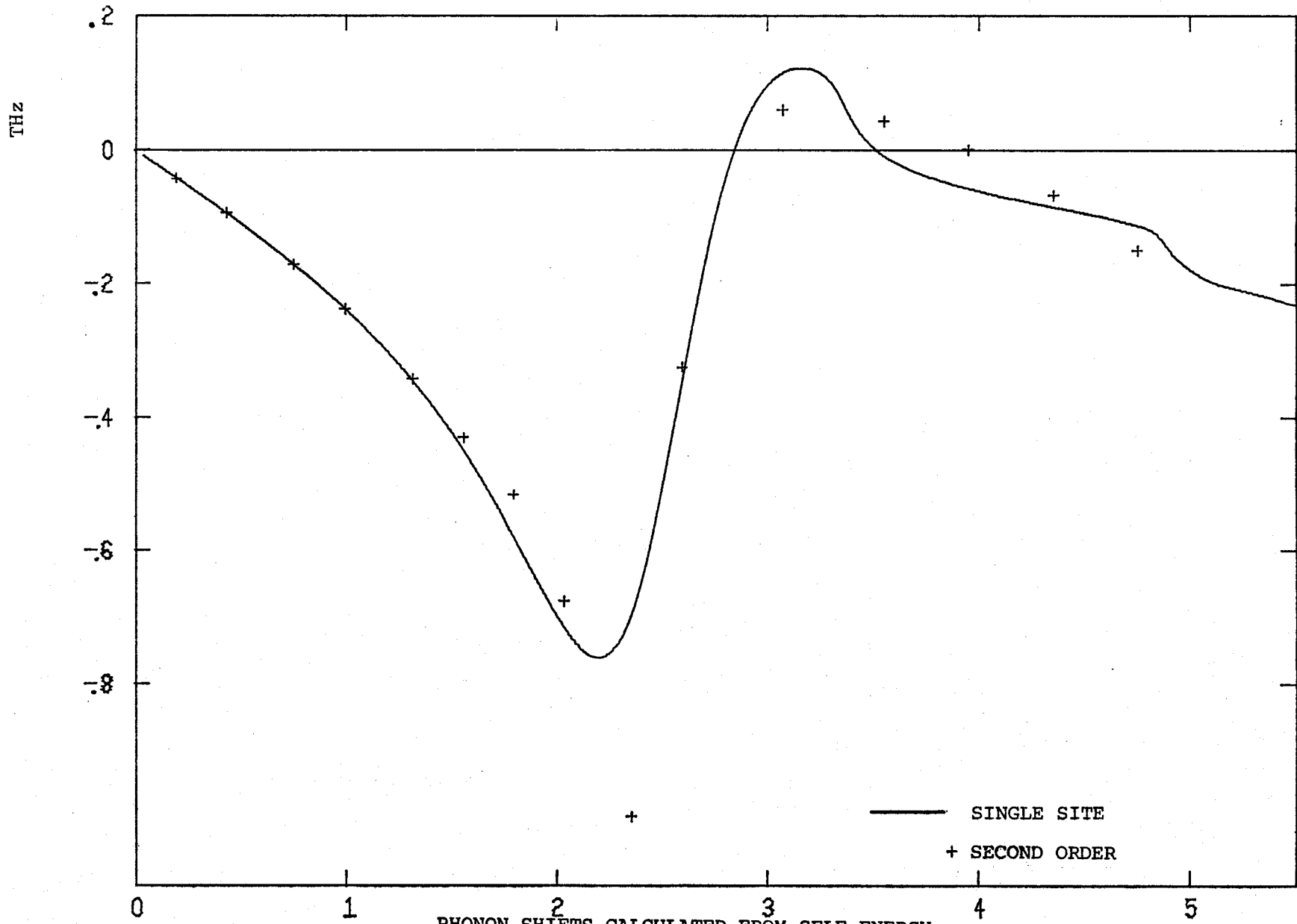
Fig. 12 PHONON SHIFTS CALCULATED FROM SELF-ENERGY AND SINGLE-SITE APPROXIMATION. L(110) c=20%
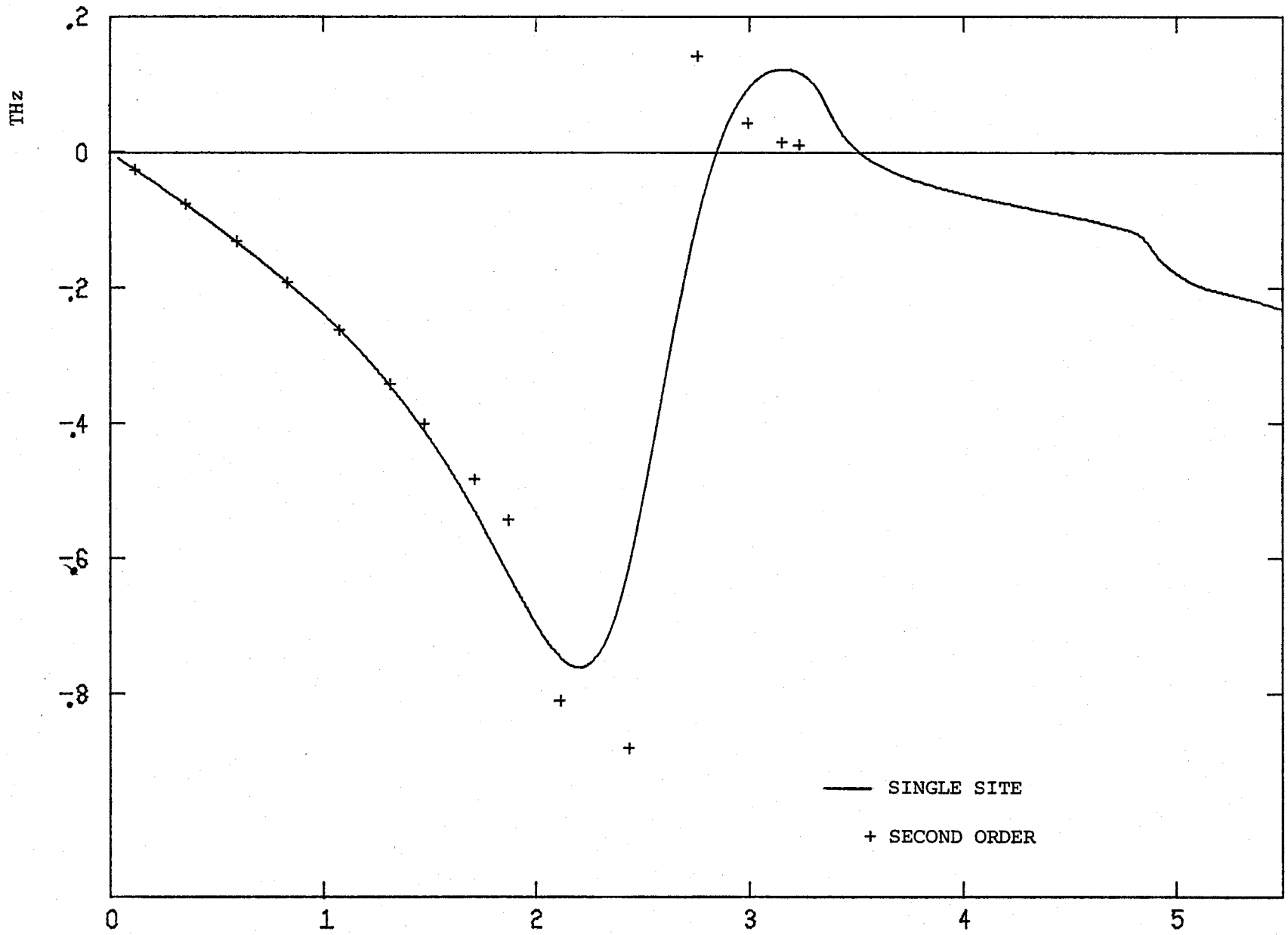
Fig. 13   PHONON SHIFTS CALCULATED FROM SELF-ENERGY
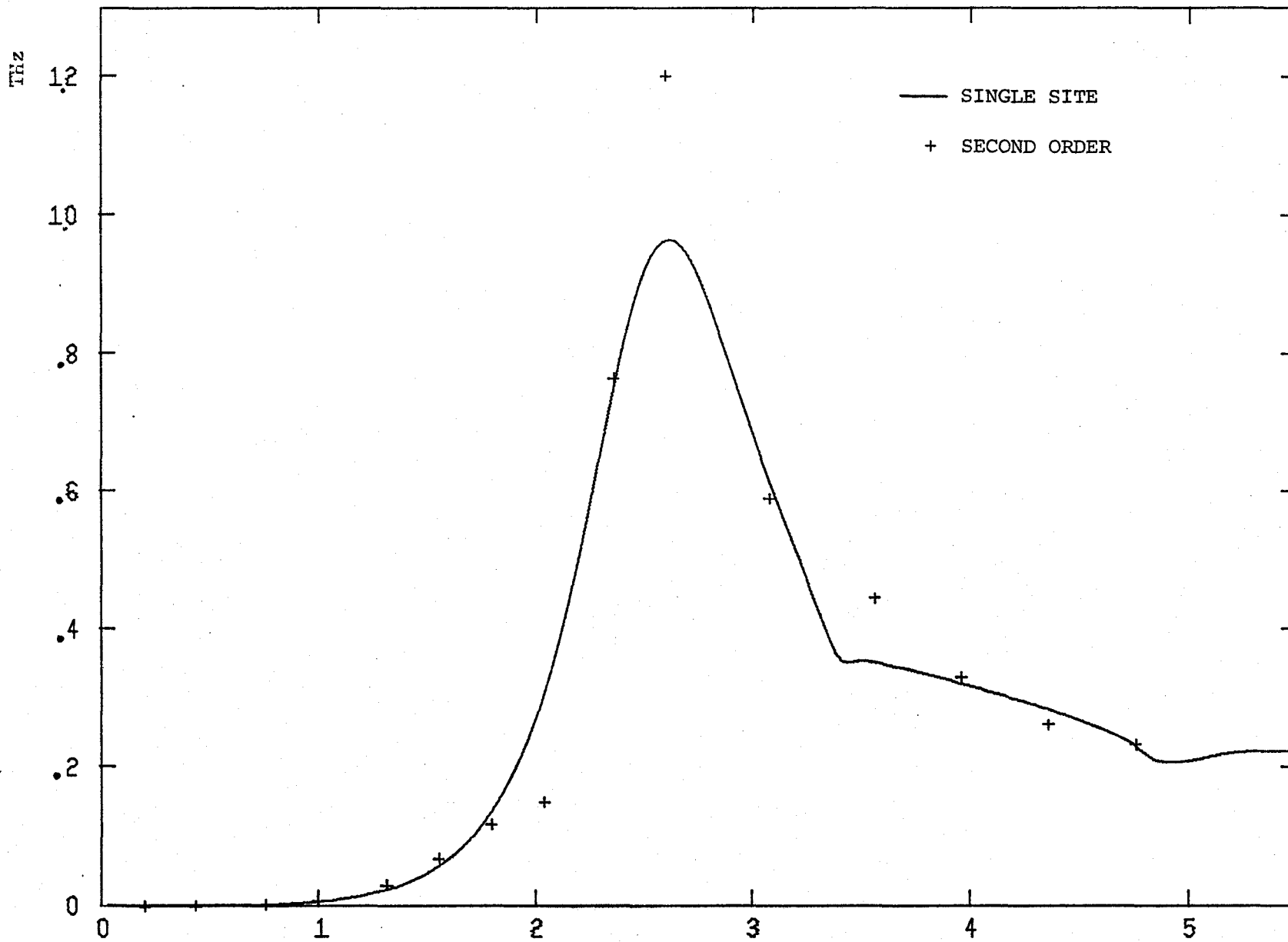
AND SINGLE-SITE APPROXIMATION T(111) c=20%

Fig. 14   PHONON WIDTHS CALCULATED FROM SELF-ENERGY
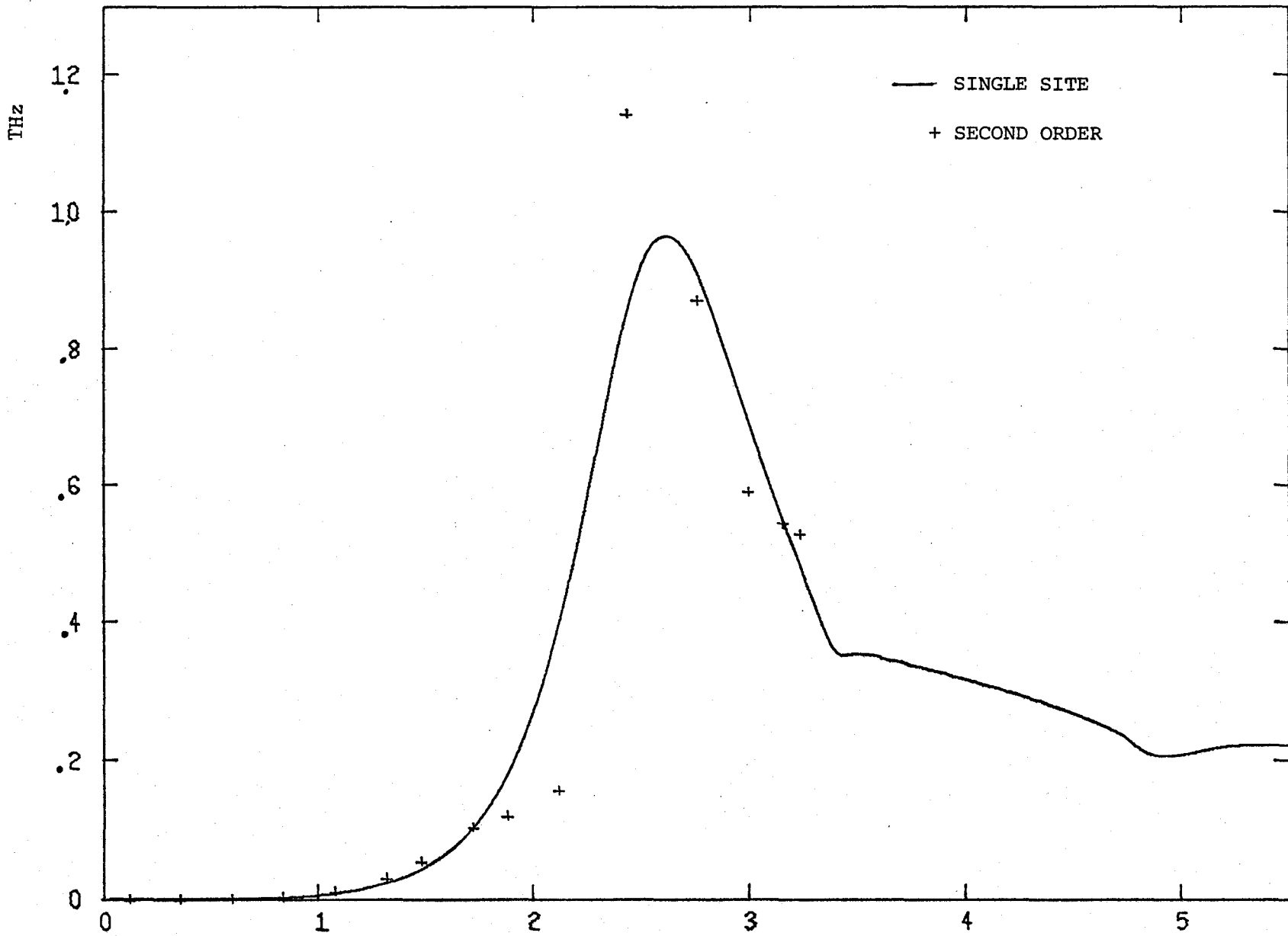AND SINGLE-SITE APPROXIMATION   L(110) c = 20%

Fig. 15   PHONON WIDTHS CALCULATED FROM SELF-ENERGY
AND SINGLE-SITE APPROXIMATION T(111) c=20%
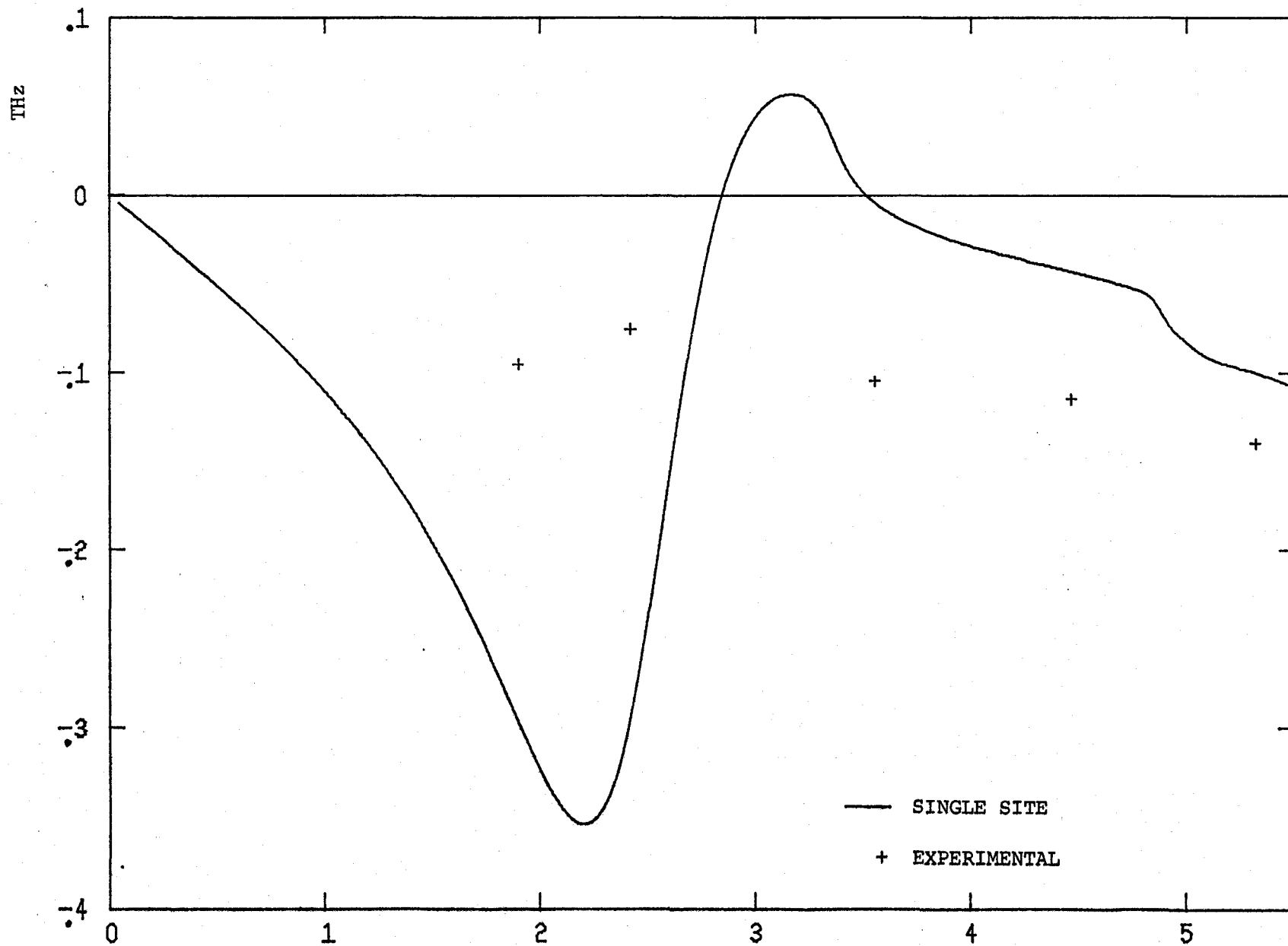
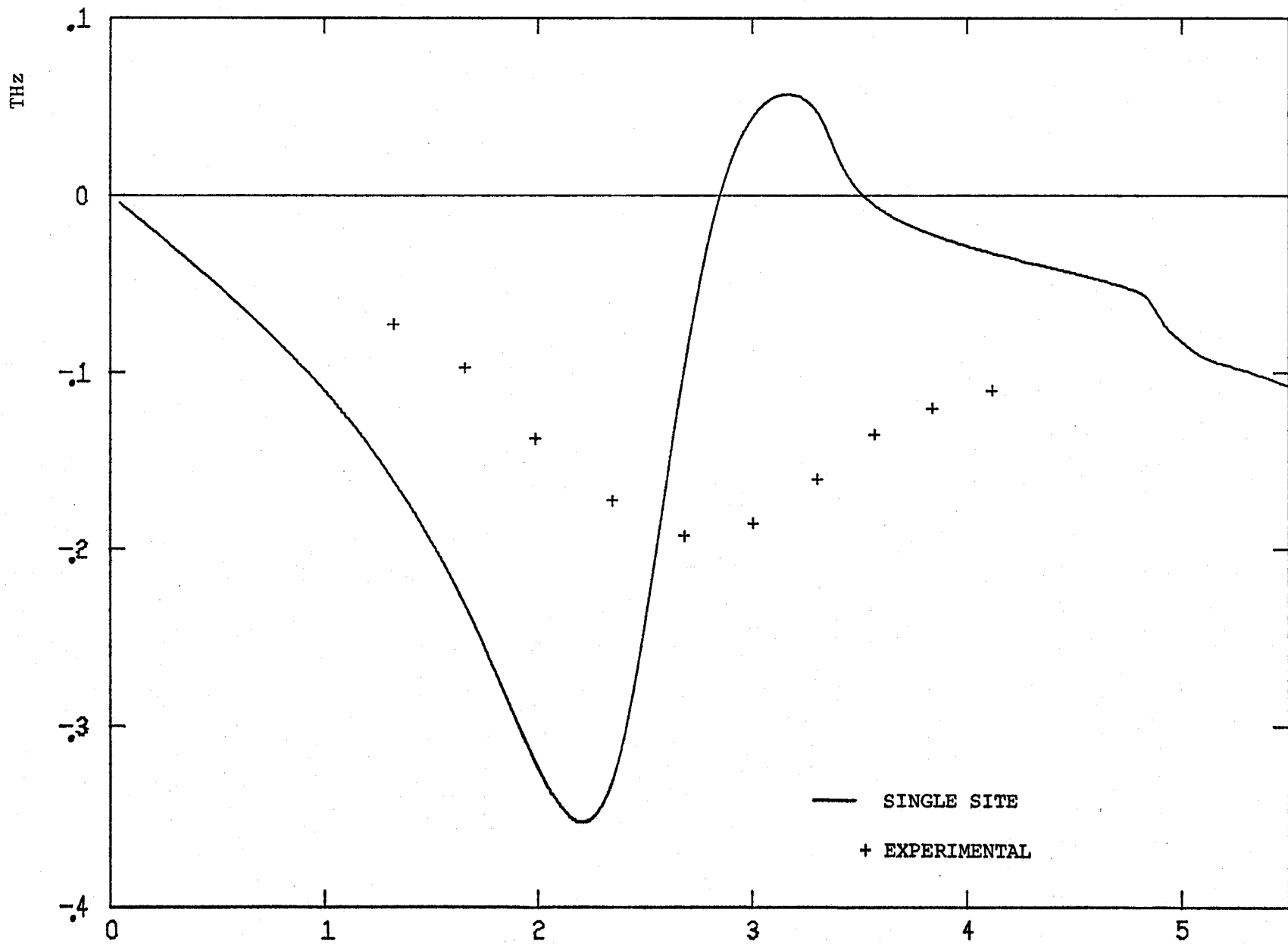Fig. 16   EXPERIMENTAL SHIFTS (SVENNSON)   L(100) c = 9.3%   THz

73

Fig. 17 EXPERIMENTAL SHIFTS (SVENNSON) $T_1(110)$ c = 9.3%

THz

74
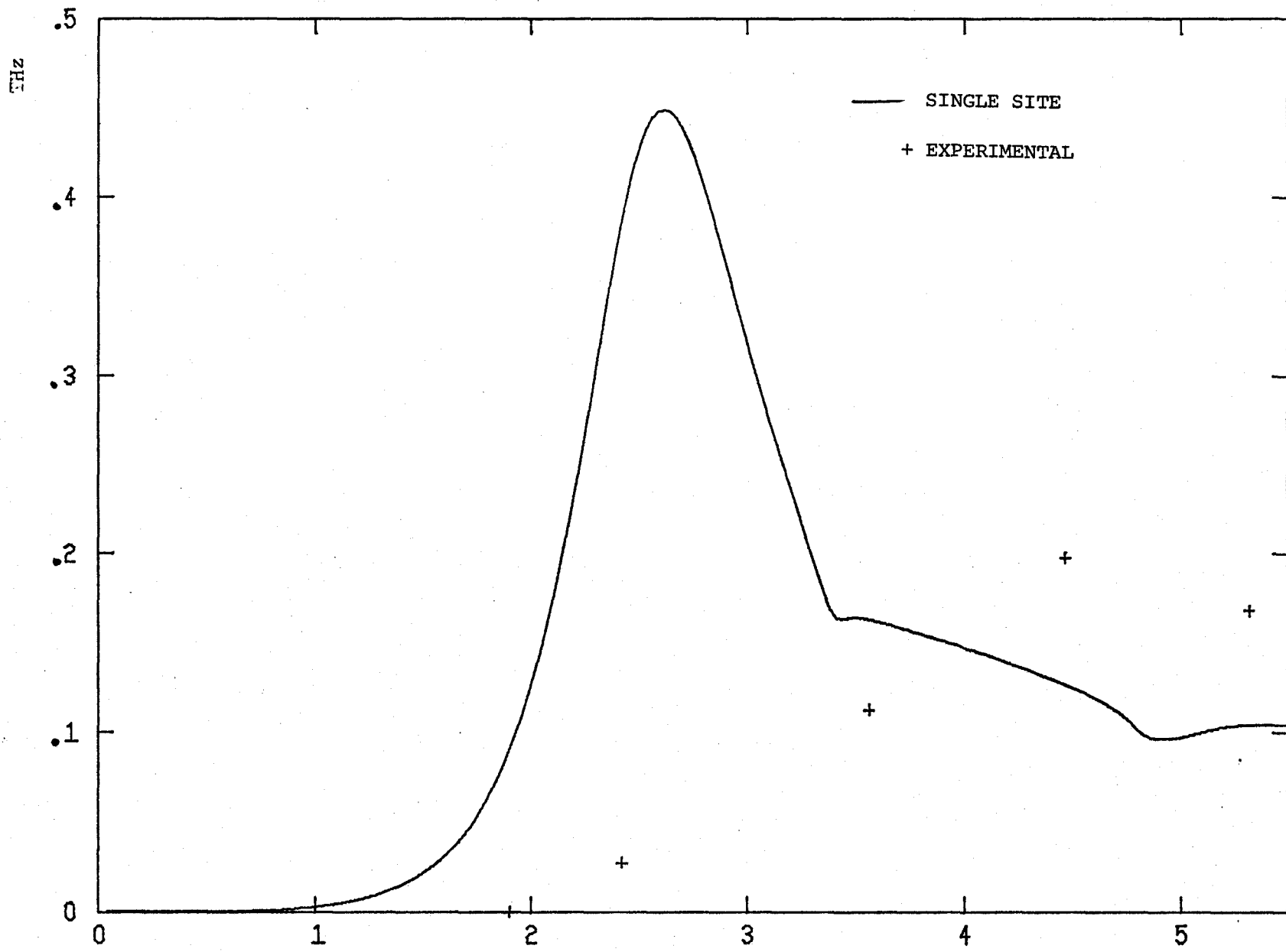
Fig. 18 EXPERIMENTAL WIDTHS (SVENNSON) L(100) c = 9.3%
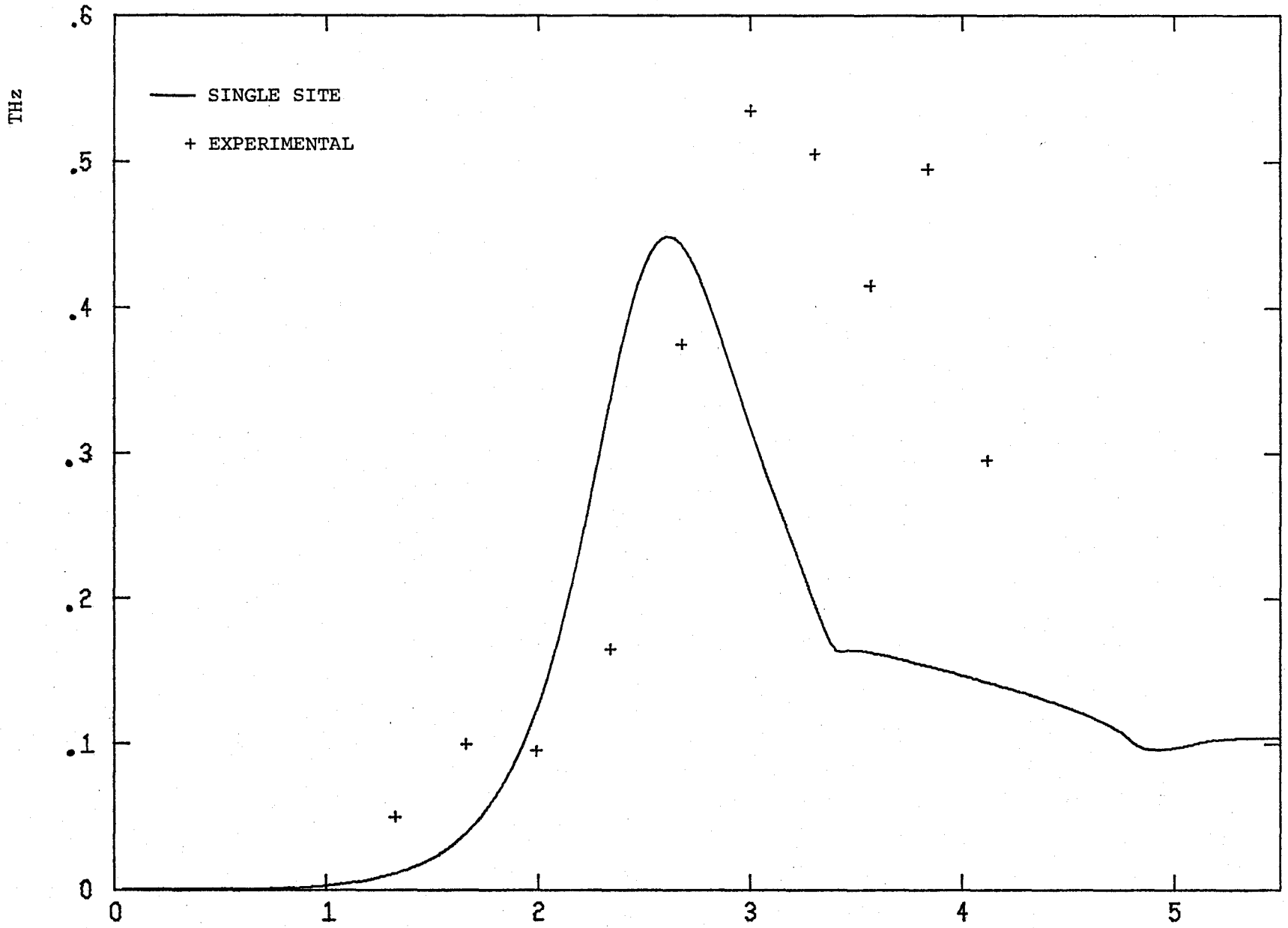
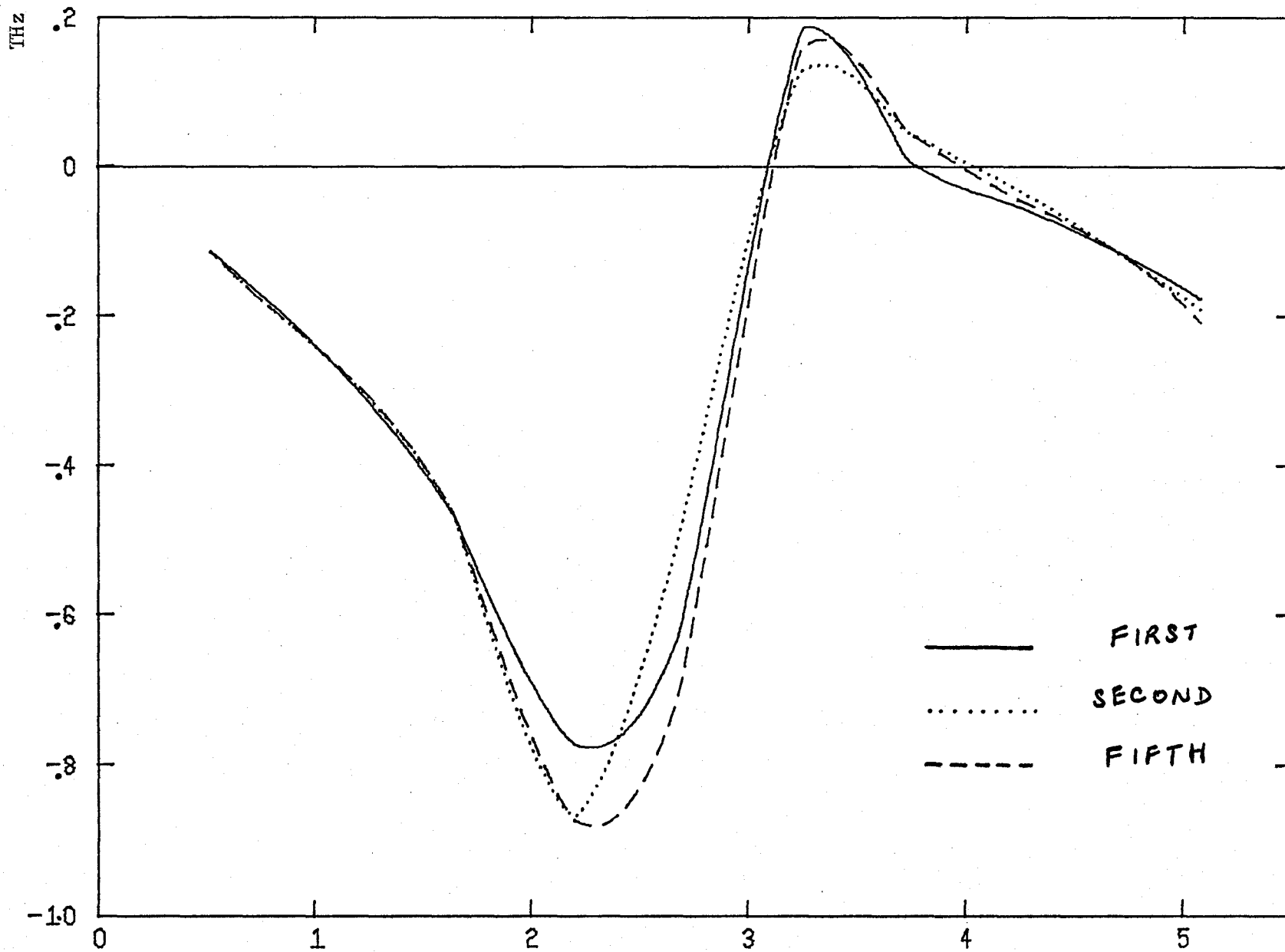Fig. 19   EXPERIMENTAL WIDTHS (SVENNSON) $T_1(110)$ c = 9.3%   THz

Fig. 20 L(111) Shifts Calculated to First, Second and Fifth Neighbour Shells.   THz

II. 5 CONCLUSIONS

The consistent result of this work has been that the interaction between neighbouring defect atoms in the harmonic, mass-defect model is extremely small. In the vibrational spectrum of a single atom, a small change was observed on adding another defect as nearest neighbour but on integrating over all frequencies to obtain the mean square displacement, the effects became less than 0.1%.

We thus expect little difference between the single-site approximation and a calculation that takes account of defect interactions. This is, in fact, the case and a calculation of phonon shifts and widths in the pair approximation at 20% impurity concentration gives a small perturbation to the single-site result, with no essentially new structure.

However the experimental results of Svensson and Kamitakahara at an impurity concentration of only 9.3% show considerable distortion from the low concentration results. Thus the mass-defect model does not take account of the important effects at reasonably high concentration.

To improve the model, the first necessary step at this point is to include changes in the force constants. Force constant changes have been included at low concentration in the single-site approximation by Bruno, Hampson and Woodside, and also by Kesharwani and Agrawal, but the extension to including pairs correctly would be extremely complicated and promises to provide a lot of work in the future.

APPENDIX

GROUP THEORY OF AN ISOLATED DEFECT PAIR

In this appendix we derive the irreducible representations of the point group according to which the symmetry modes of a defect pair, in an otherwise perfect crystal, transform.

For a nearest neighbour pair, the symmetry group is D_{2h}, whose elements are

$$(E,\ C_2^{,}\ C_2^2,\ C_2^3,\ i,\ \sigma_h,\ \sigma_v^z,\ \sigma_v^{xy})$$

where the notation is given in Fig. A.1 we first notice that the point group D_{2h} has no irreducible representations of diversionality greater than one (Tinkham (1964)) hence we expect no degenerate symmetry modes.

We proceed to construct the reducible six-dimensional representation axis of the two atoms, evaluating the characters of the associated matrices leads to the character table

D_{2h}	E	C_2^1	C_2^2	C_2^3	i	σ_h	σ_v^z	σ_v^{xy}
R	6	-2	0	0	0	0	0	2

Reducing this representation into its component irreducible representations leads to

$$R \rightarrow A_{1g} \oplus B_{2g} \oplus B_{3g} \oplus B_{1u} \oplus B_{2u} \oplus B_{3u} \qquad (A1)$$

The same process applied to the second nearest neighbour case   whose
symmetry group is D_{4h} leads to the reduction

$$D_{4h} \quad E \quad C_2=C_4^2 \quad 2C_4 \quad 2C_2' \quad 2C_2'' \quad i \quad \sigma_h \quad 2iC_4 \quad 2\sigma_v \quad 2\sigma_d$$

$$R \quad 6 \quad -2 \quad 2 \quad 0 \quad 0 \quad 0 \quad 0 \quad 0 \quad 2 \quad 2$$

$$R \rightarrow A_{1g} \oplus E_g \oplus A_{2u} \oplus E_u \; . \tag{A2}$$

Thus we see that two-dimensional irreducible representations appear,
so that two doubly degenerate symmetry modes are found.   We can now
construct projection operators to project out those functions that trans-
form according to each irreducible representation, thus giving us the
symmetry vectors for the normal modes.   These projection operators are
given by (Tinkham (1964))

$$\mathscr{P}^{(j)} = \frac{\ell_j}{h} \sum_R \chi^{(j)}(R) \; P_R \tag{A3}$$

where   j   labels the normal mode which transforms according to an
irreducible representation of diversionality ℓ_j and with respect to
which the group element R has character $\chi^{(j)}(R)$.   h is the number of
elements in the group and P_R is the operator corresponding to the group
elevent R.   For example in the second neighbour case   for the irreducible
representation E_g;

$$\mathscr{P}_{E_g} = \frac{2}{16} \{ 2 \, P_{E_g} - 2P_{C_2} + 2P_i - 2P_{2\sigma_h} \} \tag{A4}$$

$$\mathscr{P}_{E_g} z_1 = \frac{1}{8}\{2z_1 - 2(-z_1) + 2(-z_2) - 2(z_2)\} \tag{A5}$$

Thus the symmetry vector is $\frac{1}{\sqrt{2}}(00100-1)$ in a Cartesian basis. Similarly the symmetry vectors for all symmetry modes are found to be;

NEAREST NEIGHBOUR

A_{1g} $\frac{1}{2}(110-1-10)$

B_{2g} $\frac{1}{\sqrt{2}}(00100-1)$

B_{3g} $\frac{1}{2}(1-10-110)$

B_{1u} $\frac{1}{2}(110110)$

B_{2u} $\frac{1}{2}(1-101-10)$

B_{3u} $\frac{1}{\sqrt{2}}(001001)$

SECOND NEIGHBOUR

A_{1g} $\frac{1}{\sqrt{2}}(100-100)$

E_g' $\frac{1}{\sqrt{2}}(0100-10)$

E_g'' $\frac{1}{\sqrt{2}}(00100-1)$

A_{2u} $\frac{1}{\sqrt{2}}(100100)$

$$E_u^{'} \qquad\qquad \frac{1}{\sqrt{2}}(010010)$$

$$E_u^{''} \qquad\qquad \frac{1}{\sqrt{2}}(001001)$$

We now employ these symmetry vectors to transform the Green's functions to normal co-ordinates via

$$P^j(\omega) = \sum_{\alpha\beta} \sigma_\alpha^j \, P_{\alpha\beta} \, \sigma_\beta^j \qquad\qquad (A6)$$

where α and β range over the values 1 to 6. Applying this transformation for all symmetry modes we find;

NEAREST NEIGHBOUR

$$P_{A_{1g}} = P_{xx}(1,1) - P_{xx}(1,2) - P_{xy}(1,2) \qquad (a)$$

$$P_{B_{2g}} = P_{zz}(1,1) - P_{zz}(1,2) \qquad (b)$$

$$P_{B_{3g}} = P_{xx}(1,1) - P_{xx}(1,2) + P_{xy}(1,2) \qquad (c)$$

$$\qquad\qquad\qquad\qquad\qquad\qquad\qquad\qquad (A7)$$

$$P_{B_{1u}} = P_{xx}(1,1) + P_{xx}(1,2) + P_{xy}(1,2) \qquad (d)$$

$$P_{B_{2u}} = P_{xx}(1,1) + P_{xx}(1,2) - P_{xy}(1,2) \qquad (e)$$

$$P_{B_{3u}} = P_{zz}(1,1) + P_{zz}(1,2) \qquad (f)$$

SECOND NEIGHBOUR

$$P_{A_{1g}} \quad = \quad P_{xx}(1,1) - P_{xx}(1,2) \qquad \text{(a)}$$

$$P_{E_g}{}' \quad = \quad P_{yy}(1,1) - P_{yy}(1,2) \qquad \text{(b)}$$

$$P_{E_g}{}'' \quad = P_{zz}(1,1) - P_{zz}(1,2) \qquad \text{(c)}$$

$$\text{(A8)}$$

$$P_{A_{2u}} \quad = \quad P_{xx}(1,1) + P_{xx}(1,2) \qquad \text{(d)}$$

$$P_{E_g}{}' \quad = P_{yy}(1,1) + P_{yy}(1,2) \qquad \text{(e)}$$

$$P_{E_u}{}'' \quad = P_{zz}(1,1) + P_{zz}(1,2) \qquad \text{(f)}$$

BIBLIOGRAPHY

Aiyer, R.N., Elliott, R.J., Krumhansl, J.A. and Leath, P., (1969), Phys. Rev. $\underline{181}$, 1006.

Born, M. and Huang, K., Dynamical Theory of Crystal Lattices (Clarendon Press, Oxford 1956).

Bruno, R., Ph.D. Thesis, McMaster University (1971).

Churchill, R.V., Complex Variables and Applications (McGraw-Hill, 1960).

Hampton, D., M.Sc. Thesis (unpublished) McMaster University (1973).

Kesharwani, K.M. and Agrawal, B.K. (1971), Phys. Rev. B$\underline{4}$, 4623; (1972) Phys. Rev. B$\underline{5}$, 2130; (1972), Phys. Rev. B$\underline{6}$, 2178; (1973) Phys. Rev. B$\underline{7}$, 5153.

Martin, T.P., (1967), Phys. Rev. $\underline{164}$, 1151.

Nickel, B.G., and Krumhansl, A., (1971), Phys. Rev. B $\underline{4}$, 4354.

Svensson, E.C. and Kamitakahara, W.A., Can. J. Phys. (1971), $\underline{49}$, 2291.

Taylor, D.W. (1964), Thesis (unpublished); (1975) in Dynamical Properties of Solids, Eds. G. K. Horton and A. A. Maradudin (North Holland),Vol. 2, Chapter 5.

Tinkham, M. (1964), Group Theory and Quantum Mechanics, (McGraw-Hill).

Woodside, R. (1976), (private communication).

Zubarev, D.N., (1960), Sov. Phys. -Uspekhi, $\underline{3}$, 320.